Novel Approaches to Newtonian Noise Suppression in Interferometric Gravitational Wave Detection

by

Nicholas R. Hunter-Jones

Submitted to the Department of Physics
in partial fulfillment of the requirements for the degree of

Bachelor of Science in Physics

at the

MASSACHUSETTS INSTITUTE OF TECHNOLOGY

June 2011

Author .....

Department of Physics
May 20, 2011

Certified by .....

Nergis Mavalvala
Professor of Physics
Thesis Supervisor

Accepted by .....

Nergis Mavalvala
Senior Thesis Coordinator, Department of Physics

Novel Approaches to Newtonian Noise Suppression in Interferometric Gravitational Wave Detection

by

Nicholas R. Hunter-Jones

Submitted to the Department of Physics
on May 20, 2011, in partial fulfillment of the
requirements for the degree of
Bachelor of Science in Physics

Abstract

The Laser Interferometer Gravitational-wave Observatory (LIGO) attempts to detect ripples in the curvature of spacetime using two large scale interferometers. These detectors are several kilometer long Michelson interferometers with Fabry-Perot cavities between two silica test masses in each arm. Given Earth's proximity to various astrophysical phenomena LIGO must be sensitive to relative displacements of 10^{-18} m and thus requires multiple levels of noise reduction to ensure the isolation of the interferometer components from numerous sources of noise. A substantial contributor to the Advanced LIGO noise in the $1-10$ Hz range is Newtonian (or gravity gradient) noise which arises from local fluctuations in the Earth's gravitational field. Density fluctuations from seismic activity as well as acoustic and turbulent phenomenon in the Earth's atmosphere both contribute to slight variations in the local value of g. Given the direct coupling of gravitational fields to mass the LIGO test masses cannot be shielded from this noise. In an attempt to characterize and reduce Newtonian noise in interferometric gravitational wave detectors we investigate seismic and atmospheric contributions to the noise and consider the effect of submerging a gravitational wave detector.

Thesis Supervisor: Nergis Mavalvala
Title: Professor of Physics

Acknowledgments

I would like to thank Prof. Nergis Mavalvala for her encouragement, support, and understanding as a thesis advisor and for making my experience in physics at MIT as positive as it was. Furthermore I would like to thank her for making my experience in both experimental physics classes 8.13 and 8.14 as positive as it was. I would also like to thank Rai Weiss for coming up with the submerged detector concept.

Lastly I would like to thank my parents for nurturing my interest in science from an early age and for their continued support and encouragement in pursuing what I love. Never did they utter a word of discouragement. To my parents, Ian and Lynette, and my sister Bridget, I owe everything.

Contents

List of Figures

Chapter 1

Introduction

The Laser Interferometer Gravitational-wave Observatory's purpose is the detection of gravitational waves. These waves are fluctuations in the fabric of spacetime radiated by accelerating mass, a phenomenon predicted by Einstein's General Theory of Relativity. However only large scale astrophysical phenomena, like black hole binaries or supernovae, can generate detectable gravitational waves on Earth and still these fluctuations are incredibly faint. The theoretical strain, given the Earth's proximity to nearby binaries and the average rate of supernovae, here on Earth is 10^{-21}. LIGO's aim is to detect these ripples using two large scale interferometers with multiple levels of noise reduction to ensure the isolation of the interferometer components from the many sources of noise on the Earth's surface. The LIGO interferometers are 4 km in length and thus to detect a signal a sensitivity of 10^{-18} m is required. To do this the mirrors and stages of the interferometer must be kept extremely still which requires a number of levels of feedforward and feedback control, suspension of components, and even squeezing the laser light. For active damping the system requires high precision, low noise displacement sensors.

Clearly the largest motivation for gravitational waves detectors is the direct detection and thus direct observation of gravitational waves. Once detailed detections and analysis of gravitational wave becomes possible not only could the predictions of general relativity be verified but could provide a more detailed view and possibly reveal aspects of gravity's not predicted in the classical theory, for example the exis-

tence of a scalar field that arises with the graviton field in various theories of quantum gravity. More realistically the successful detection of gravitational waves will give us a great deal of information regarding astrophysical phenomenon that are currently not well understood, such as the dynamics of supernovae, black hole radiation, and dark matter, but more generally will give a new perspective on observing the skies. Since it's beginning astronomy has been the study of celestial objects by interpreting light. All of the information we get regarding stars, for example, their rotation, composition, age, etc., is from the light they emit. Gravitational waves offer a new insight, allowing us to study dynamics and structure of matter in these astrophysical objects. The reason the information is different is because gravitational waves are emitted by the entire system, bulk motions, and not atom and electrons as is the case with light. Information from these bulk motions can provide valuable insight into the dynamics and structure of astronomical systems.

Detection of gravitational radiation is the only way to directly observe and thus verify the existence of black holes given that semiclassical radiation, Hawking radiation, has an observable strength far less than that of gravitational waves. Moreover gravitational waves interact weakly with matter neither attenuating or scattering when passing through close-set distributions of matter and thus can pass through dense star systems without losing information. It is for this reason that we also might get a chance to gain information about stars and objects obscured by brightest and densest parts of the Milky Way.

1.1 Motivation

As we will discuss in depth later, there are many noise sources that contribute to LIGO's noise spectrum, as is to be expected when one is concerned with length scales one thousand times smaller than a proton. The noise source we are primarily concerned with is Newtonian noise contributions in the 1-10 Hz region. LIGO has reached sensitivities below 10^{-21} but only at relatively high frequencies. Many know sources of gravitational waves in the universe have been shown to radiate at amplitude

of 10^{-19} to as high as 10^{-14}, but only at very low frequencies and far below the LIGO cutoff. At frequencies lower than 10 Hz the noise becomes dominated by seismic noise and Newtonian noise. Seismic noise is easier to deal with as it can be shielded against, but Newtonian noise couples directly the the test masses. This is why space based detectors like LISA are appealing because in space seismic and gravity gradient noise would be far less prevalent. But if we were able to reduce the contributions of Newtonian noise in next generation gravitational wave detectors, where substantial improvements in seismic isolation have been realized then we would open up ground based interferometric detectors to lower frequencies. This becomes apparent in Figure 1-1. Signals from white dwarf binaries and black hole binaries fall just below the limit. Additionally neutron star - neutron star binaries produce signals that go as $f^{-8/3}$ and would become detectable with improvements in low frequency noise.

In this thesis we will present an overview of general relativity and gravitational wave physics, then methods of detection of gravitational waves. Then we will look at the LIGO detector and the various sources of noise and how they can be isolated against. We will then present the calculations and estimations of seismic and atmospheric noise in interferometric detectors. After building up the necessary formalism we will consider the atmospheric Newtonian noise in a submerged detector as well as the implications for seismic Newtonian noise.

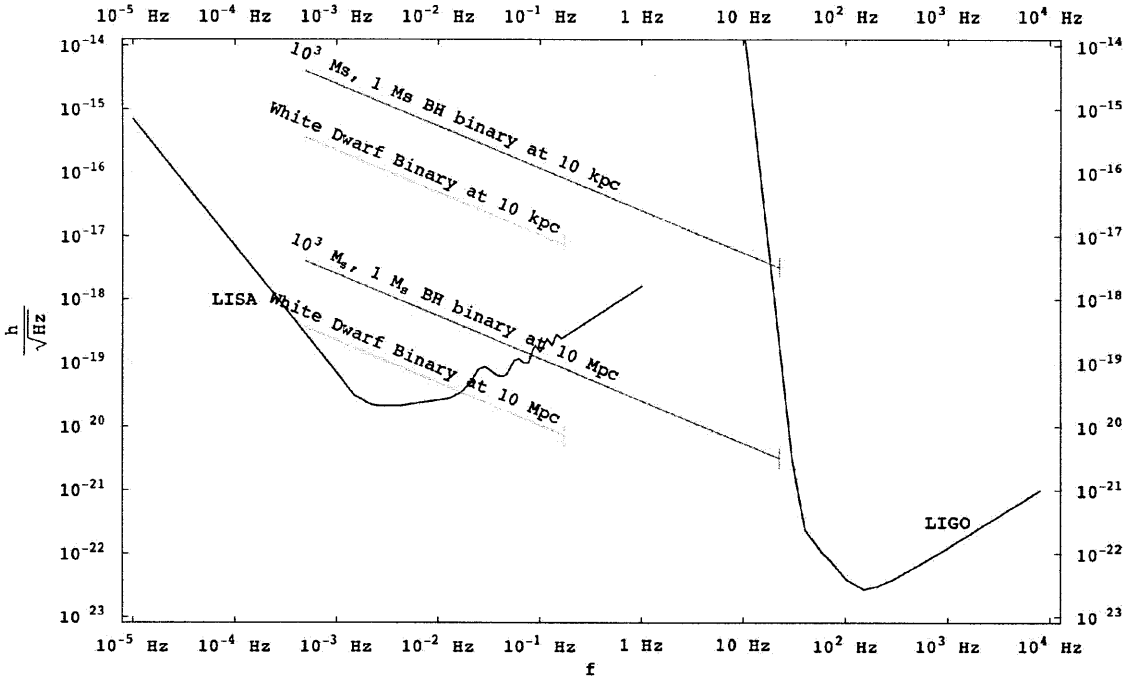

Figure 1-1: The theoretical sensitivities of Advanced LIGO and LISA plotted with the expected strains from a few astrophysical sources. Modified from [9]

Chapter 2

Gravitational Waves and Gravitational Wave Detectors

2.1 General Relativity

General relativity is currently the best description of gravitation in modern physics. The theory was first formulated by Albert Einstein from 1905 to it's completion in 1915, and finally published in 1916. General relativity is a generalization of Einstein's previous theory of special relativity and Newton's gravitation to non-Euclidean geometries, thus providing a unified description of gravitation as a geometric property of four dimensional spacetime. Since 1915 the theory has been remarkably successful in providing an understanding of astrophysical phenomena and making unexpected predictions that has since been scientifically verified. Such phenomena, which stood in opposition to Newtonian physics, include gravitational time dilation, gravitational red shift, and Shapiro time delay. The first and one of the most successful triumphs of general relativity was the accurate explanation of the perihelion advance of Mercury. General relativity's predictions have been confirmed by all experiments and observations to date. It stands as one of the most successful theories in modern physics. The theory also makes more abstract predictions of seemingly bizarre astrophysical phenomenon. For example, it implies the existence of black holes, regions of spacetime so distorted that even light cannot propagate out. Additionally, most

cosmological models of a constantly expanding universe are predictions of general relativity. Another of general relativity's predictions, most relevant to this paper, is that of gravitational waves. Gravitational waves are the perturbation of the metric, the curvature of spacetime, propagating as a wave outwardly from a source. We will now briefly go through the fundamentals of general relativity and the derivation of gravitational radiation.

The theory is best understood in two parts; the distribution of matter tells spacetime how to curve, and the curvature tells particles how to move. General relativity, like Maxwell's description of electromagnetism, is a classical field theory, but the field is not a physical concept that exists in space but is the shape of the spacetime itself. A description of a gravitating system under general relativity is a mathematical description of the geometry of spacetime, as general relativity is a geometric theory. In the theory spacetime is represented by a four dimensional Lorentzian manifold described by a metric $g_{\mu\nu}$. A Lorentzian manifold is an important special case of a pseudo-Riemannian manifold where the metric need not be positive definite. Now we comment briefly on the convention used in this section; here we are using the metric signature $(-,+,+,+)$, all Greek indicies run from zero to three spacetime dimensions whereas Latin indicies run from one to three spatial dimensions, and in the relevant formulae in this section we work in units where $c = 1$. Introducing a local coordinate system x^{μ} we then start with the Einstein field equations, which are typically written in the form

$$G_{\mu\nu} = 8\pi G T_{\mu\nu} \tag{2.1}$$

where G is Newton's gravitational constant, $T_{\mu\nu}$ is the stress-energy tensor, a description of the distribution of matter in space, and $G_{\mu\nu}$ is a symmetric second-rank tensor that acts on the metric, typically called the Einstein tensor. The Einstein tensor is subsequently defined as

$$G_{\mu\nu} = R_{\mu\nu} - \frac{1}{2} g_{\mu\nu} R \quad \text{where} \quad R_{\mu\nu} \equiv R^{\alpha}_{\mu\alpha\nu} \quad \text{and} \quad R \equiv g^{\mu\nu} R_{\mu\nu} \tag{2.2}$$

where $R_{\mu\nu}$ is the Ricci tensor, a contraction of the Riemann tensor $R_{\alpha\beta\mu\nu}$, and R is the

Ricci scalar, a further contraction using the metric. For completeness the Riemann tensor is defined as

$$R^{\alpha}_{\beta\mu\nu} = \partial_\mu \Gamma^{\alpha}_{\nu\beta} - \partial_\nu \Gamma^{\alpha}_{\mu\beta} + \Gamma^{\alpha}_{\mu\lambda}\Gamma^{\lambda}_{\nu\beta} - \Gamma^{\alpha}_{\nu\lambda}\Gamma^{\lambda}_{\mu\beta} \tag{2.3}$$

where $\Gamma^{\sigma}_{\mu\nu}$ is the Christoffel connection. The connection in a mathematical object that encodes information about parallel transport. Thus given some curved surface, or more generally a manifold, we can determine how a set of basis vectors change as they are moved around the manifold. More specifically parallel transport is a way of transporting information regarding the geometry of the space along smooth curves. We can see then how information about the curvature of a space, i.e. the Riemann tensor, can be expressed entirely in terms of Christoffel symbols and their first partial derivatives. The Christoffel symbol can be expressed explicitly in terms of the metric tensor,

$$\Gamma^{\sigma}_{\mu\nu} = \frac{1}{2} g^{\sigma\rho}(\partial_\mu g_{\nu\rho} + \partial_\nu g_{\rho\mu} - \partial_\rho g_{\mu\nu}). \tag{2.4}$$

2.2 Gravitational Wave Physics

To probe the structure of spacetime and further explore the implications of general relativity we will take a weak field approximation. Assume the metric is close to that of flat spacetime

$$g_{\mu\nu} = \eta_{\mu\nu} + h_{\mu\nu} \tag{2.5}$$

where $h_{\mu\nu}$ is a small perturbation, i.e. $|h_{\mu\nu}| << 1$, and the Minkowski metric takes the canonical form $\eta_{\mu\nu} = \text{diag}(-1, +1, +1, +1)$. We now evaluate the Einstein tensor for this perturbed field and find the linearized equation

$$G_{\mu\nu} = \frac{1}{2}(\partial_\sigma \partial_\nu h^{\sigma}_{\mu} + \partial_\sigma \partial_\mu h^{\sigma}_{\nu} - \partial_\mu \partial_\nu h - \Box h_{\mu\nu} - \eta_{\mu\nu}\partial_\mu \partial_\nu h^{\mu\nu} + \eta_{\mu\nu}\Box h) \tag{2.6}$$

where $\Box$ is the D'Alembertian operator. While general relativity is clearly a classical field theory it is more interesting to note that it is a gauge theory, where the gauge

field is spacetime itself. The quantization of this gauge field is the gauge boson for gravity, but this is another story. We know that a gauge theory must be gauge invariant or else it losses it's physical significance. Proper justification of the theory's gauge invariance would require discussion about diffeomorphisms of metric spaces. Assuming this is so we can choose a gauge specified by $\Box x^\mu = 0$, which is equivalent to $g^{\mu nu}\Gamma^\rho_{\mu\nu} = 0$. In the weak field limit this becomes

$$\partial_\mu h^\mu_\lambda - \frac{1}{2}\partial_\lambda h = 0. \tag{2.7}$$

This gauge is commonly referred to as the Einstein gauge. In this gauge the field equations take on the elegant form

$$\Box h_{\mu\nu} - \frac{1}{2}\eta_{\mu\nu}\Box h = -16\pi G T_{\mu\nu}, \tag{2.8}$$

and the vacuum equations $R_{\mu\nu} = 0$ take on the even simpler form

$$\Box h_{\mu\nu} = 0, \tag{2.9}$$

a familiar form for a relativistic wave equation. These two equations describe waves propagating at the speed of light. The fact that it's form has a natural dependence on the coordinate system raised significant doubts regarding the validity of gravitational waves. Many thought that the waves were just a result of a coordinate transformation and were note anything physical. Although we can, in fact, eliminate the gravitational forces by choosing an appropriate gauge we can not transform to a gauge where the tidal forces are not present, indicating that the phenomena is physical. We will not go through the tedious derivation of the two polarization states for gravitational waves, which can be found in [5] and [30]. We will briefly show that two polarization states should exist. Given a coordinate system in our gauge x^μ, we can always induce coordinate changes $x'^\mu = x^\mu + \zeta^\mu$ and the system unchanged in this gauge if $\Box\zeta^\mu = 0$. This indicates that h can have as many as two degrees of freedom. In a vacuum $T_{\mu\nu} = 0$ we can introduce the transverse-traceless gauge where $h_{\mu 0} = 0$, $h_{ii} = 0$, and

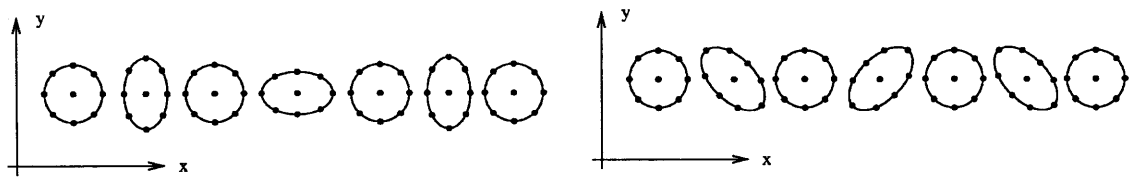

Figure 2-1: On the left, the effect of a "+" polarized gravitational wave on a ring of particles over time, and on the right the effect of a "x" polarized gravitational wave. Modified from [5].

$\partial_j h_{ij} = 0$. In this gauge we can write the Riemann curvature tensor as

$$R_{0i0j} = \frac{1}{2}\partial_0\partial_0 h_{ij}. \tag{2.10}$$

Since the Riemann tensor is gauge invariant this implies that the weak field, and thus the gravitational wave, has two and only two degrees of freedom, and thus there are two polarization states of the wave. The two polarizations are shown in Figure 2-1.

To first motivate and provide validity to the above weak field limits in General Relativity and it's prediction of gravitational radiation before we motivate direct detection of gravitational waves let's briefly discuss the agreement of these predictions with the famous binary system PSR1913+16. In 1974 Russell Hulse and Joseph Taylor discovered that this system was losing energy in almost exact agreement with the predicted gravitational radiation of the system.

We know from General Relativity that a mass quadrupole moment that changes with time can produce gravitational radiation, analogous to the electromagnetic radiation produced by oscillating electric or magnetic quadrupoles. We can consider certain types of gauge transformations which leave certain global quantities invariant, most importantly the total energy on a surface S of constant time. We can take this and consider the total energy radiated through to infinity ΔE and subsequently perform many lengthy calculations to find the radiated power, $\Delta E = \int P dt$, in terms of the quadrupole moment of a radiating source. Such calculations are done in [5]

and [30] but here we will merely quote the result

$$P = \frac{G}{45}\left(\frac{d^3Q^{ij}}{dt^3}\frac{d^3Q_{ij}}{dt^3}\right) \tag{2.11}$$

where Q_{ij} is the traceless part of the quadrupole moment. This is the radiated power due to gravitational radiation of a gravitating system with a quadrupole moment. The traceless quadrupole moment for a binary system is derived by integrating the energy density T^{00} of the binary. Doing this and taking the third derivative we find

$$P = \frac{128}{5}GM^2r^4\Omega^6 = \frac{2}{5}\frac{G^4M^5}{r^5} \tag{2.12}$$

where M is the mass of each of the objects in the binary, r the radius from the center of mass, and Ω the orbital frequency, which we find by equating forces in classical mechanics.

The binary system PSR1913+16 consists of a pulsar in orbit with a neutron star which each follow elliptical orbits about a common center of mass. Both stars are relatively small and thus orbit according to Kepler's laws, so our classical treatment of the orbits was valid. The period of the orbit is 7.75 hours, which is incredibly small by astrophysical standards, and since a pulsar serves as an accurate clock astronomers can track the change in the orbital period as the system radiates energy. It turns out the energy lost by the system was in agreement with the predicted energy loss due to gravitational radiation of such a binary system disagreeing by 0.2%. An interesting note, recent analysis has shown that the 0.2% discrepancy is due to poorly known galactic constants. In 1993 Hulse and Taylor were awarded the Nobel Prize for their discovery, the only Nobel prize for gravitational wave related physics to date.

2.3 The Detection of Gravitational Waves

Hulse and Taylor's discovery of the radiating binary system strongly motivated general relativity and the accuracy of gravitational wave physics but nevertheless does not constitute direct detection of gravitational waves. A gravitational wave detector

exploits the effect of a passing gravitational wave on matter. As we recall from our discussion in 2.2 a propagating gravitational wave's primary effect is to change the relative distance between adjacent free particles. Thus in principle one could construct a gravitational wave detector that measured the distances between free particles. Even more naively one could imagine creating gravitational waves in a laboratory and eliminating the dependence on cataclysmic astrophysical phenomenon, but a simple calculation using Equation 2.12 negates such a possibility. The quadrupole formula for the radiated power of an object is dependent on M, r, and Ω, choosing the limiting rotational velocity of the object to be the speed of sound, the radius to be on the order of a kilometer and the mass to be 10^6 kg, a huge, massive object rotating incredibly fast, still only corresponds to a power of 10^{-15} watts, which only gets worse as this power is converted into the flux one would expect from a detector in the vicinity of the rotating object.

Since constructing a gravitational wave source on Earth is inconceivable we must turn to the cataclysmic astrophysical phenomena as potential sources. The first attempt at gravitational wave detection were resonant bar detectors. The instruments consisted of heavy metal cylinders in which gravitational waves would drive a mechanical oscillation of the bar itself. Transducers mounted at the ends of the resonating bar would thus transform the oscillations to electrical pulses. The extremely low amplitude of gravitational waves and thus the signal in the system results in an incredibly small signal to noise ration. To help overcome this the signal to noise is improved by time integration of the first normal mode oscillation of the bar. These detectors exploit the sharp resonance of the resonating cylinder to get their sensitivity. Unfortunately the sensitivity of the bar detectors in confined to a very narrow bandwidth, perhaps a few Hertz, about the resonant frequency. In general for these devices $\delta f/f \approx 10^{-3}$. These were the first practical instruments developed for gravitational wave detection, largely because the technology necessary for interferometric detectors was fairly undeveloped in the 1960's and 1970's.

The first of these bar detectors were developed by Joesph Weber in the 1960's, subsequently publishing papers with evidence that he had successfully detected grav-

itational radiation. In the 1970's the results of Weber's experiments were largely discredited, although Weber continued to argue that he had been successful in detecting gravitational waves. Other attempted to reproduce his results by building similar apparatuses with no success. Additionally the device he had constructed, which used non-cryogenic aluminum bars, was not nearly sensitive enough. Regardless his work is considered pioneering and generated generations of interest in gravitational wave detection. Since Weber's work, the construction of bar detectors has been greatly improved. A gravitational wave of $h \sim 10^{-21}$ makes a $L \sim 3$ m bar detector vibrate with an amplitude 10^{-21} m. The main noise sources include thermal noise, which in a cryogenic system contributes vibrations on the order of 10^{-18} m, although using a high Q, resonating material could lower this to $\sim 10^{-20}$. This is largely why Weber's initial design was thought to be flawed as it operated at room temperature. Sensor noise arises from the transducer's conversion of mechanical oscillation to electrical signal and the amplification of the signal to record it. Quantum noise arises from the zero point vibrations in the bar detector, which for a resonant frequency of 1 kHz are on the order of 5×10^{-21}. No squeezing techniques have been developed for bar detectors as they have in quantum optics.

Thus resonant bar detectors remain fairly narrow bandwidth detectors with much difficulty in pushing below sensitivities of 10^{-21}, although recent proposals to use spheres at the resonating mass make claims of possible sensitivities below the previous limit. But with their narrow bandwidth they remain suitable for specific high frequency searches.

In the 1970's Rainer Weiss and others developed the idea of using an interferometer as a gravitational wave detector. Laser interferometer gravitational wave detectors are essentially Michelson interferometers, measuring the differential length change between test masses and subsequently the difference in length of the two orthogonal arms. The beam is split and sent down the two arms, reflected and recombined resulting in an interference pattern. Any relative change in the lengths of the orthogonal arms will cause a change in the interference pattern. A diagram of the basic optical layout is shown in Figure 2-2. In principle, if the test masses are in free fall then the

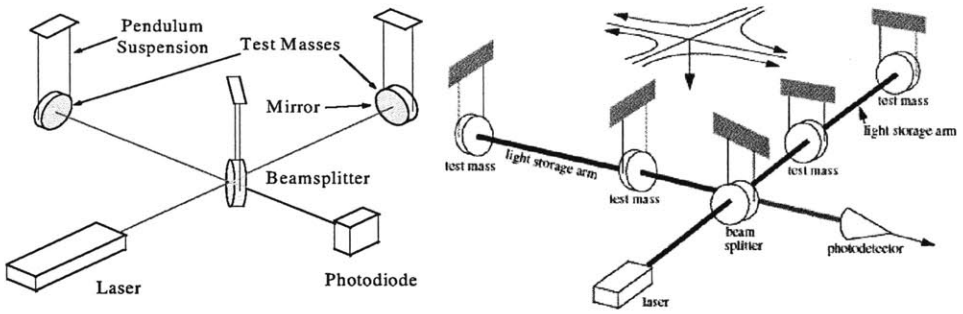

Figure 2-2: On the left: Basic optical schematic of an interferometric detector. Modified from [23]. On the right: Optical schematic used by the current LIGO detectors. Modified from [27].

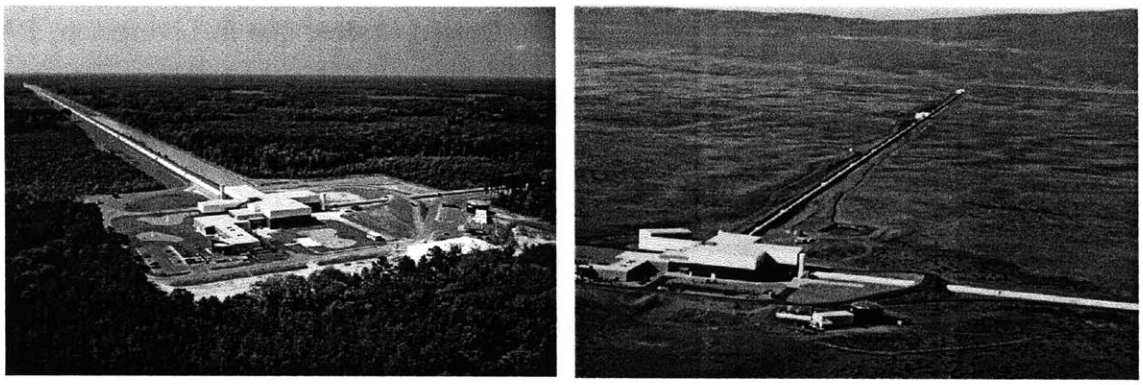

Figure 2-3: On the left: An aerial view of the LIGO Livingston Observatory in Livingston, LA. On the right: An aerial view of the LIGO Hanford Observatory in Hanford, WA. Both taken from [27].

changes in the interference pattern correspond directly to changes in the curvature of spacetime, and thus the passage of a gravitational wave. As we saw in our description of gravitational waves the wave has an orthogonal effect on the plane of it's propagation. In an interferometer this would manifest as one arm becoming longer and the other proportionally shorter. Clearly a ground based detector would not be in freefall but instead would be coupled to the motions of the Earth, but isolation from these forces would allow successful detection. There are many other noise sources that inhibit successful detection as we will discuss shortly. But unlike bar detectors, interferometric detectors offer the possibility of high sensitivities over a wide range of frequencies.

2.4 Laser Interferometer Gravitational-wave Observatory

The Laser Interferometer Gravitational-wave Observatory (LIGO) one of the leading gravitational wave detection efforts along with VIRGO, GEO, TAMA, and AIGO. LIGO has two 4 km long interferometer in the United States, one in Livingston, LA and the other in Hanford, WA (where an additional 2 km interferometer is operated in parallel to the first). Aerial views of the LIGO sites are shown in Figure 2-3. Many universities around the world are involved in the LIGO Scientific Collaboration (LSC), with primary research groups at MIT and CalTech. Since the theoretical gravitational wave strain on Earth is 10^{-21}, the amplitude of the wave LIGO is attempting to detect is on the order of $\delta\ell_{gw} \sim h\ell \sim 10^{-18}m$. As previously described the LIGO detectors are essentially Michelson interferometers using coherent light and an optical readout to determine the difference in the arm lengths from the interference of the beams. LIGO uses a NdYAF laser with a wavelength $\lambda = 1064$ nm and a photodiode to measure the phase difference. Since the time light takes to travel up and down the arm is only 10^{-5} sec, which is much less than a gravitational wave period, the light in each arm is stored in a Fabry-Perot optical resonant cavity using partially transmissive input mirrors. The effective path length of the light is thus increased by a factor of 100. Initial LIGO used 25 cm, 11 kg, fused silica, test masses whereas Advanced LIGO will use 34 cm, 40 kg, fused silica, test masses, which we will see plays an important role in reducing noise. In addition to improved seismic isolation systems the Advanced LIGO test masses will be suspended from a quadruple pendulum. The strain sensitivities achieved in the first five LIGO runs are shown in Figure 2-4. With it's many improvements Advanced LIGO should push the noise floor even lower and hopefully to sensitivities capable to detecting gravitational waves.

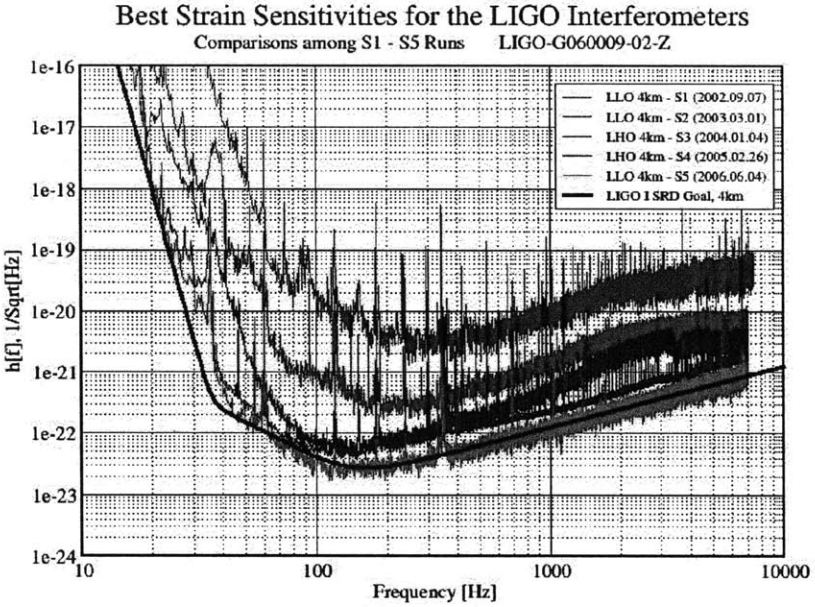

Figure 2-4: Best strain sensitivities for Initial LIGO, Science Runs: S1 through S5. Taken from [27].

2.5 Noise in Interferometric Detectors

In this section we will discuss the primary sources of noise that appear in interferometric gravitational wave detectors and limit sensitivity. In naive consideration of a interferometric detector one would imagine that most noise sources would be negligible, and that a sufficiently isolated system should suffice. But given the scale of the gravitational wave signal one must consider a vast number of noise sources that rarely pose problems in experiments. In ground based interferometric detectors, the most important limitations to sensitivity result from the effects of seismic noise and other disturbances that propagate through the Earth, thermal fluctuations in the interferometer itself, in the test masses and suspensions systems, shot noise, high frequency quantum noise in the photodiodes, radiation pressure noise, low frequency quantum noise from photon momenta in high powered lasers, and finally gravity gradient noise, the primary focus of this thesis, arising from minor fluctuations in Newtonian gravitational fields. The current estimates for relevant Advanced LIGO noise contributions are shown in Figure 2-5. A brief discussion, based on [?] [23] and [31], of each of these noise sources follows:

Seismic Noise

Noise is introduced from seismic activity in the Earth, mechanical oscillations from human activity (i.e. highways, construction work, etc.), natural phenomenon in the atmosphere, and many other forms of ground born oscillations. These external vibrations are eliminate with passive and active damping systems. Simple pendulum systems provide a relatively simple way to isolate the system from external noise affecting the test masses in the horizontal plane. The transfer function of a pendulum, concerning the horizontal motion of the mass at the suspension pointy, falls off as $1/f^2$ above the pendulum resonance, thus isolating from high frequency vibrations. Since there is undoubtedly coupling of horizontal noise in the vertical axis, we must also screen out vertical oscillations. We can isolate the test mass from vertical noise in a similar way by suspending it on a spring. In order to further isolate the system around the pendulum and spring resonant frequencies we must also incorporate active damping. Additionally low frequency isolation must take place in order to prevent low frequency seismic noise from inducing motion in the test masses. Low frequency isolation takes different forms in different detectors, but in Advanced LIGO this is done using seismometers and actuators to reduce via feedback control and thus servo-control out the seismic noise. The full Advanced LIGO seismic isolation system consists of a variety of active and passive stages of isolation. There is an external hydraulic isolation system (HEPI), two stages of active isolation in-vacuum (ISI) with passive spring and flexure systems coupling the stages, completed by a quadruple pendulum test mass suspension.

Thermal Noise

Thermal noise is caused by temperature fluctuations, inducing minor expansions and contractions in the test masses and suspension systems contributing a significant source of low frequency, sensitivity limiting, vibrational noise. As with seismic noise, the noise is further amplified by the bouncing of light between the mirrors. Thermal noise in the pendulum suspensions, corresponding to resonant frequencies, is around

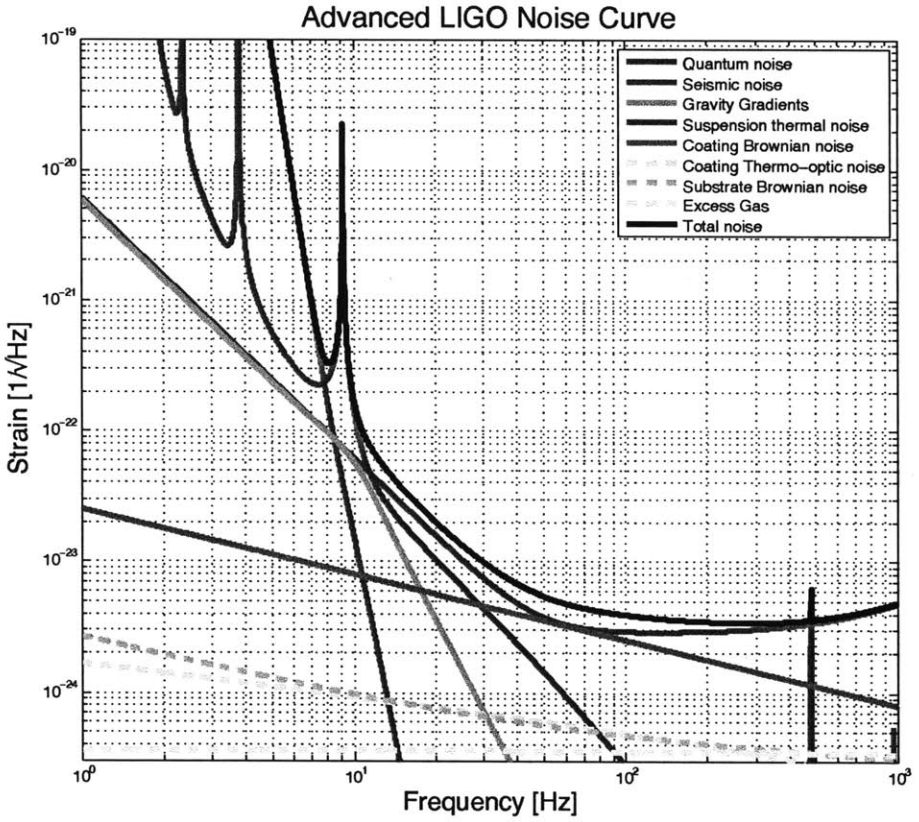

Figure 2-5: Current estimates for the noise contributions in Advanced LIGO. Figure generated by the GWINC (Gravitational Wave Interferometer Noise Calculator) package in MATLAB [28].

a few Hz, and internal vibrations of the mirror from thermal noise have natural frequencies of several kHz. In order to keep the thermal noise as low as possible we ensure that the masses and pendulum resonances have very high Q values, and thus the loss factor of the resonances is as low as possible, as then we can confine the vibrational energy from the noise to a small bandwidth around the resonant frequency. Furthermore we must ensure that the test masses have a shape such that the frequencies of the internal resonances are kept as high as possible. It is interesting to note that we can see the confined resonances in the thermal noise Figure 2-5. Another type of thermal noise arises from losses within the mirror's dielectric coating, generating fluctuations in the phase shift of the reflected light. Since fluctuation dissipation is closely related to Brownian motion this specific effect is often termed coating Brownian noise

Advanced LIGO uses 40 kg, 34 cm diameter, fused silica test masses [27].As no lossy materials should come into contact with the test masses they are suspended by fused silica blocks, which in turn are suspended by fused silica fibers. This setup allows the test masses to have quality factors exceeding 10^7.

Shot Noise

Shot noise is a type of electronic noise that occurs when a finite number of particles that carry energy five rise to statistical fluctuations in some measurement. Since the beam with which interferometry is done is quantized, i.e. composed of photons, the photons arrive at a detector at random and make random fluctuations in the light intensity. Since this is a Poisson process, the signal to noise ratio is $N/\sqrt{N} = \sqrt{N}$, and thus the error improves as the square root of the number of photons. Of course, the more photons used, the less shot noise contributes to the signal. It turns out that to achieve the required sensitivity we need a laser operating at a wavelength of 10^{-6} m providing a power of 6×10^6 W at the input to a Michaelson interferometer. This large laser power mandated of us is far beyond the output of any continuous laser, but this problem is overcome using light-recycling techniques to use the light efficiently. A more detailed analysis of shot noise and light recycling is discussed in

[15] and [23].

Radiation Pressure Noise

Although shot noise is a quantum noise, there are a number of other effects that constitute 'quantum noise', including radiation pressure noise. As the laser power is increased this noise source becomes more important arising from fluctuations in radiation pressure. One interpretation is that the beam splitter divides up the photons constituting laser light randomly. If each is scattered randomly and independently then we get a distribution of N photons in each arm with a $\sim \sqrt{N}$ noise in radiation pressure. A more detailed description can be attributed to vacuum fluctuations in the photon fields with respect to amplitudes. With this in mind we can state that radiation pressure noise arises from uncertainty in the amplitude of the photon fields in the interferometer laser while shot noise arises from uncertainty in the phase of the photons. These correspond to a sensitivity limit called the Standard Quantum Limit (SQL) which corresponds to Heisenberg's uncertainty principle. Methods to achieve and even overcome the SQL have been implemented in Advanced LIGO by putting the laser light in a squeezed state. We will not attempt to successfully describe the process of squeezing light, but the basic idea is that just as an uncertainty principle exists between position and momentum, as does one between energy and time, and thus amplitude and phase of light. Since in gravitational wave detection we are concerned primarily with phase, we can inject noise in the amplitude and achieve greater certainty in phase. More detailed descriptions of quantum noise locking and poderomotive squeezing can be found in [7] and [16].

Gravity Gradient Noise

The last noise source which test masses cannot be shielded from is Newtonian, or gravity gradient, noise. This noise arises from fluctuations in the local Newtonian gravitational field induced by seismic activity or atmospheric turbulence. A test mass in a detector will respond to the changes in gravitational field just as it would respond to gravitational waves. A diagram depicting the effect of a varying

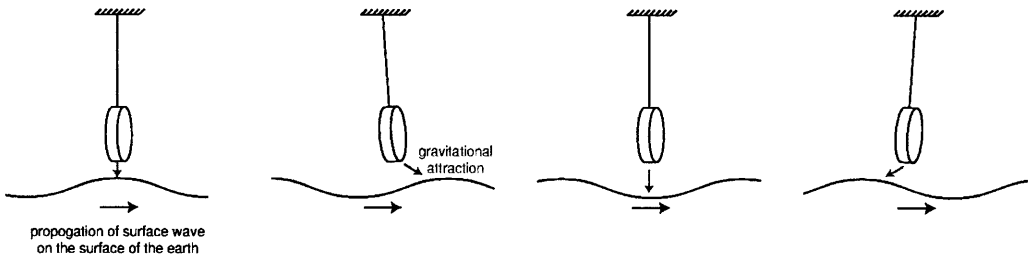

Figure 2-6: Depiction of the induced fluctuations in the local gravitational field on a test mass by the propagation of a passing seismic wave. Modified from [23].

gravitational field on a test mass in shown in Figure 2-6. Seismic waves and other surface phenomenon change the density in the Earth around the detector and these mass fluctuations constitute noise in the detector. Similarly acoustic and turbulent phenomenon in the atmosphere cause changes in air pressure and thus in air density also constituting Newtonian noise. Although the spectrum does fall off sharply with increasing frequency it still dominates in below 10 Hz. As next-generation gravitational wave detectors are constructed and new technology is implemented we will see significant improvement in many of the aforementioned noise sources. Unfortunately improvements with respect to gravity gradient noise in ground based detectors are less likely to occur. Gravity gradient noise will likely continue to dominate and limit the sensitivity of LIGO in the 1-10 Hz region. The most promising approach to detecting gravitational waves at frequencies lower than 1 Hz is space based interferometers like LISA.

Chapter 3

Newtonian Noise in Gravitational Wave Detectors

As previously discussed Newtonian noise, also termed gravity gradient noise, is noise due to fluctuating Newtonian gravitational forces that induce motion in the test masses of the gravitational wave detector. Gravity gradients were first identified as a potential noise source in an interferometric gravitational wave detector by Rainer Weiss in 1972. The first analytical estimates of Newtonian noise were done by Peter Saulson in 1984 [25]. Newtonian noise arises primarily from two sources, seismic Newtonian noise where gravity gradients are induced by ambient seismic activity and atmospheric Newtonian noise where gravity gradients arise from acoustic and turbulent phenomenon. In his paper Saulson gives a rudimentary estimation of gravity gradients generated by seismic noise, atmospheric noise, and a third source, moving massive bodies. The current estimates for seismic gravity gradient noise, which are used in the Advanced LIGO noise curves, are done by Hughes and Thorne [13]. The current estimates for atmospheric gravity gradient noise are given in [8] and [4]. We will now give a more detailed overview of each Newtonian noise source as well as the theoretical description and estimation of the characteristic noise curve itself.

3.1 Seismic Gravity Gradient Noise

When ambient seismic waves pass near or directly beneath a LIGO detector, they give rise to density perturbations in the Earth itself. When the density of the Earth is altered slightly, the local gravitational field will alter slightly, changing the local value of g, the acceleration of gravity. These fluctuating Newtonian gravitational forces induce motion in the LIGO test masses. Gravity gradient noise is most pronounced, with respect to LIGO sensitivities, at $f \lesssim 20$ Hz and thus contributes most to the LIGO noise spectrum in the 1 Hz to 10 Hz range, see Figure ??. We can isolate the test masses from seismic activity using many levels of active and passive damping and isolation but even in principal one cannot isolate the system from Newtonian noise because gravitational forces cannot be shielded (without the advent of negative gravitational charge in the gravitational analog of a Faraday cage). From our knowledge of seismic and atmospheric phenomenon we can estimate the strength of gravity gradient noise. We will now outline the work of Hughes and Thorne [13] in describing the seismic activity contributing to the Newtonian noise with respect to the LIGO sites and the derivation of the transfer function $T(f)$ used to describe the gravity gradient noise from ambient seismic activity.

Before we continue we will briefly outline some important details regarding seismic waves that are relevant to the following description of Newtonian noise. Seismic waves are low-frequency acoustic waves that most noticeably result from cataclysmic geophysical phenomenon but are also caused by many other natural and anthropogenic sources. The latter are referred to ambient vibrations, the cause of the relevant background Newtonian noise. There are two types of seismic waves, body waves and surface waves. Body waves travel through the Earth's interior, reflected and refracted by the differences in density and modulus. The two types of body waves are primary P-waves, compressional waves that are longitudinal in nature, and secondary S-waves, shear waves that are transverse in nature. P-waves propagate faster than S-waves, up to velocities of 5000 m/s. Surface waves, on the other hand, travel along the Earth's surface; the two types of Surface waves are Rayleigh waves, surface waves that travel

as ripples analogous to water waves, and Love waves, surface waves that cause circular shearing of the ground.

Now we continue with our description of Newtonian noise. In keeping with LIGO notation and expressing noise transfer functions in frequency space, we define the gravity gradient noise transfer function $T(f)$ to be

$$T(f) \equiv \frac{\tilde{x}(f)}{\tilde{W}(f)}, \tag{3.1}$$

the transfer function of $\tilde{x}(f)$, the displacements in the test masses, to $\tilde{W}(f)$, motions in the Earth produced by seismic activity. A simple and elegant form of this transfer function is derived in [25]. Given the importance of this result and the reliance of the work done by Hughes and Thorne, and subsequently the LIGO for Newtonian noise, we will outline the derivation. Gravitational forces accelerate the test masses with an acceleration of $\omega^2 x$, since we are interested in working in the frequency domain. Consider a simplified interferometric gravitational wave detector and a region in the neighborhood of the interferometer that exhibits fluctuations in it's mass due to seismic activity, a diagram of the simplified detector is shown in Figure 3-1. The time dependent fluctuations experienced in the massive region are $\Delta M(t) = M(t) - \langle M(t) \rangle$, and thus the force experienced by the test mass of mass m due to this perturbation is

$$\vec{F}(t) = m\frac{G\Delta M(t)}{r^2}\mathbf{e}_r. \tag{3.2}$$

We may consider the force in the x-direction with respect to the coordinate system in the diagram and transform the equation into the frequency domain

$$F_x = m\frac{G\Delta M(\omega)\cos\theta}{r^2}. \tag{3.3}$$

LIGO test masses are passively isolated in vacuum with a spring and flexure system and suspended from a quadruple pendulum. We may consider the test masses as having a resonant frequency ω_0 and damping time τ. Since the force from an oscillator

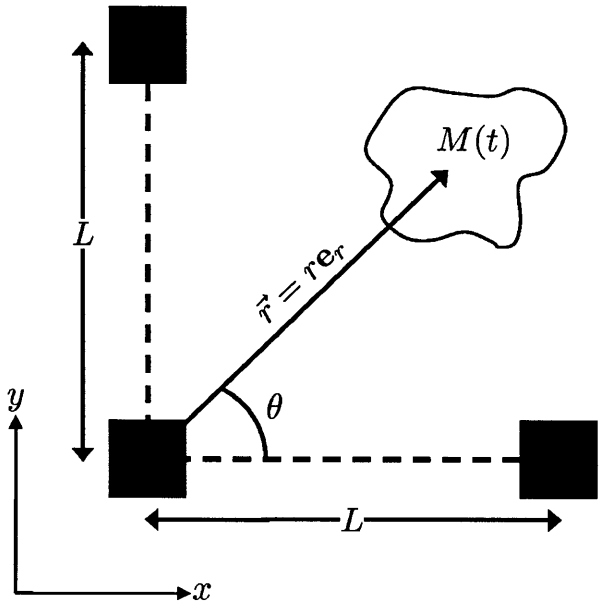

Figure 3-1: A simplistic interferometric gravitational wave detector configuration with arm length L and a nearby region of fluctuating mass $M(t)$.

is $F = m\omega^2 x$ we substitute and take the magnitude and find

$$\left((\omega^2 - \omega_0^2)^2 + \omega^2/\tau^2\right)|x(\omega)|^2 = G^2|\Delta M(\omega)|^2\frac{\cos^2\theta}{r^4}. \tag{3.4}$$

We now consider the area around our interferometer configuration to be filled with regions of fluctuating mass. The calculation we preformed above was for a coherently fluctuating region of mass $M(t)$. To achieve a computation that includes multiple coherently fluctuating regions there must be some scale at which a region is coherent. We may make the assumption that such a region is of the order $\lambda/2$ where $\lambda = v_s/f$ is the acoustic wavelength and v_s is the speed of sound of the associated seismic wave. We also need to make a second assumption that the mass fluctuations in different coherent regions are uncorrelated and are completely independent physical events. This means that we may add the the forces exerted by the coherent regions in quadrature. We are also considering the region the fluctuations are occurring in to be a homogeneous half-space, euclidean three-space bifurcated into two half-spaces by a plane, i.e. a homogeneous planar model of the earth. Since we may add the forces in quadrature the total contribution reduces to a summation of the $\cos^2\theta/r^4$

over all coherent regions in the euclidean half-space. It is reasonable to approximate this summation as an integral over θ and r, as is justified in both [25] and [13]. Thus we find

$$\sum \frac{\cos^2\theta}{r^4} \approx \frac{1}{\lambda}\int_{r_{min}}^{\infty}\int_{0}^{2\pi} \frac{\cos^2\theta}{r^4} d\theta dr \tag{3.5}$$

where we have introduced an inner cutoff radius to ensure the integral in convergent. The fact that the integral is divergent is indicative of the dominance of local gravitational fluctuations, as expected. We choose $r_{min} = \lambda/4$, the radius of our approximated coherent region. A choice of a smaller r_{min} would disregard our earlier assumption that the summation over coherent regions may be approximated as an integral. Performing the integral with the specified cutoff radius we find

$$\sum \frac{\cos^2\theta}{r^4} \approx \frac{64\pi}{3\lambda^4} = \frac{4\omega^4}{3\pi^3 v_s^4}. \tag{3.6}$$

Plugging this back into Equation 3.4 we find

$$\left((\omega^2 - \omega_0^2)^2 + \omega^2/\tau^2\right)|x(\omega)|^2 = \frac{4G^2}{3\pi^3 v_s^4}\omega^4 |\Delta M(\omega)|^2. \tag{3.7}$$

This equation tells us the force exerted on a test mass by local gravitational fluctuations and an interferometric gravitational wave detector measures the difference in the separations between test masses. For example using the configuration in Figure 3-1 the detector itself measures the difference between the interferometer x arm length and interferometer y arm length. When performing the integral above we realized that the forces induced by mass fluctuations around a test mass are largely dominated by the local fluctuations, i.e. the contributions from coherent regions on the order of a distance λ from the test mass.

The P-wave and S-wave velocities, as measured at the Livingston LIGO site and cited in [13], are 440 m/s and 220 m/s respectively. Since the frequency range of the gravitational gradients we are concerned with is 1-10 Hz, this corresponds to wavelengths, λ, of 440 m to 44 m, as we are considering the most disruptive seismic interference. The LIGO arm length is $L = 4$ km and thus we may make the

approximation $\lambda << L$. Since we argued that Newtonian noise in the test masses is dominated by coherent regions within a few wavelengths λ we may claim that the noise in the test masses is uncorrelated and thus adds in quadrature. The gradients in the difference in interferometer arm lengths is four times that of an individual test mass. To find $T(f)$ all we need to do now is express the mass fluctuation $|\Delta M(\omega)|$ as a displacement of a point on the Earth's surface from equilibrium by a passing seismic wave $|\Delta X(\omega)|$. From [25] we find that

$$|\Delta M(\omega)|^2 = \frac{\pi \rho_e^2 \lambda^4}{16} |\Delta X(\omega)|^2 = \frac{\pi^5 v_s^4 \rho_e^2}{\omega^4} |\Delta X(\omega)|^2 \tag{3.8}$$

where ρ_e is the local density of the Earth. Substitution of the previous equation into Equation 3.7, expressing the test mass displacement $|x(\omega)|$ as a differential displacement between the test masses $|\Delta x(\omega)|$, and accounting for the noise from each test mass added in quadrature we find

$$\left((\omega^2 - \omega_0^2)^2 + \omega^2/\tau^2\right) |\Delta x(\omega)|^2 = \frac{16\pi^2 G^2 \rho_e^2}{3} |\Delta X(\omega)|^2. \tag{3.9}$$

The displacements in the test masses $\tilde{x}(f) = |\Delta x(\omega)|$ and motions in the Earth produced by seismic activity $\tilde{W}(f) = |\Delta X(\omega)|$. We have thus arrived at the gravity gradient transfer function $T(f)$

$$T(f) = \frac{4\pi G \rho_e}{\sqrt{3((\omega^2 - \omega_0^2)^2 + \omega^2/\tau^2)}} \tag{3.10}$$

We will assume that we can ignore the resonant frequency $\omega_0 = \pi$ rad/s and damping time $\tau \sim 10^8$ s for frequencies $f \gtrsim 1Hz$ and that the arm length is long enough that the short wavelength approximation is valid. Then $((\omega^2 - \omega_0^2)^2 + \omega^2/\tau^2)|\Delta x(\omega)|^2 \approx \omega^4 |\Delta x(\omega)|^2$. Which gives us

$$T(f) = \frac{G\rho_e}{\sqrt{3}\pi f^2}. \tag{3.11}$$

Following [13] we define a dimensionless correction $\beta(f)$ referred to as the reduced transfer function. In the derivation we just did and that in [25] we had $\beta(f) = 1/\sqrt{3}$

which arises from the inner cutoff radius we decided upon. Thus we can imagine that a more rigorous treatment of the regions of fluctuating mass and the coherent lengths of these regions would produce a different cutoff with a different order of λ. Expressed as such the transfer function is

$$T(f) = \frac{G\rho_e}{\pi f^2}\beta(f). \tag{3.12}$$

A more rigorous treatment would have to consider the types of seismic waves and modes experienced at the test masses as well as the standard seismic activity around the test masses at each of the sites. Only after performing such an analysis could we accurately determine the reduced transfer function. The work of Hughes and Thorne in [13] does such an analysis by considering the fundamental Rayleigh and Love modes in relation to anisotropy ratios to derive and justify $\beta(f)$. Specifically see Appendix A of [13]. We will not go into their analysis of seismic modes at LIGO sites but we will note one part of their derivation that is of interest regarding the correlation of noise at the test masses. Each seismic mode will contribute to the transfer function and since the phases of these modes are uncorrelated we find the modes contribute in quadrature

$$\beta(f)\sqrt{\sum_J \omega_J \beta_J(f)^2}, \tag{3.13}$$

where the index J sums over the relevant modes. As shown in Appendix A of [13] we can express the reduced transfer function of a mode to be $\beta_J = \gamma_J \Gamma_J \beta'_J$. What we are interested in is the dimensionless function $\gamma_J(f)$ which accounts for the correlation between the Newtonian noise experianced at two different test masses. Specifically, for the two corner test masses γ will be a function of the phase shift in traveling from one mass to the other, $\gamma(\omega\ell/v_p)$ where ω is the seismic wave frequency, ℓ is the distance between the test masses, and v_p is the phase velocity of the wave. The function $\gamma(x)$ is given by

$$\gamma(x) \equiv \sqrt{1 + \frac{1}{2\pi}\int_0^{2\pi} \cos\phi \sin\phi \cos\left(\frac{\cos\phi + \sin\phi}{\sqrt{2}}x\right) d\phi} \tag{3.14}$$

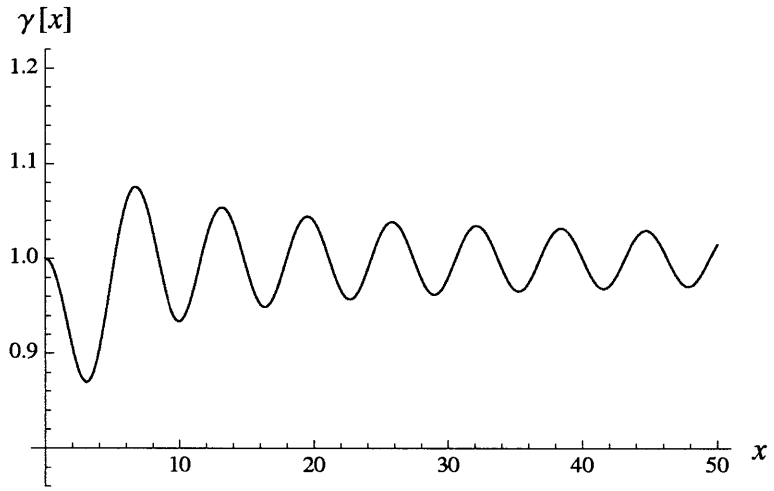

Figure 3-2: Plot of $\gamma(x)$ which accounts for the correlations of seismic Newtonian noise in the two corner test masses.

as shown in [13]. We plot the function in Figure 3-2 and observe that regardless of seismic wave properties determining ω and v_p the correlation is still on the order of unity. Much to our surprise we find that in fact for seismic Newtonian noise the noise experienced at the corner test masses is to a very good approximation uncorrelated and thus the naive assumption we made in our derivation turns out to be fairly accurate.

For completeness, in our expression for β_J, Γ_J describes the attenuation of the noise due to the height h of the test masses above the Earth's surface $\Gamma_J = \exp(-\omega H/v_{pJ})$. For the LIGO test masses $H \approx 1.5$ m and since Rayleigh and Love modes propagate on the order of a few hundred m/s we can approximate Γ_J to unity and therefore $\beta_J \simeq \beta'_J$. We present a table of reduced transfer functions predicted for the Livingston and Hanford LIGO sites contrasted with our original $\beta = 1/\sqrt{3}$ in Appendix A. We conclude by expressing Equation 3.12 as a strain $\tilde{h}(f)$ as a function of the ground noise $\tilde{x}(f)$

$$\tilde{h}(f) = \frac{G\rho_e\beta}{L\pi}\frac{1}{f^2}\tilde{x}(f), \tag{3.15}$$

where L is the interferometer arm length. To find the ground motion we first reported amplitude spectral densities of the ambient earth motion in [10]. The ground motion measured is as such, between 0.1 Hz and 10 Hz $\tilde{x}(f)$ is proportional to $1/f^2$. This

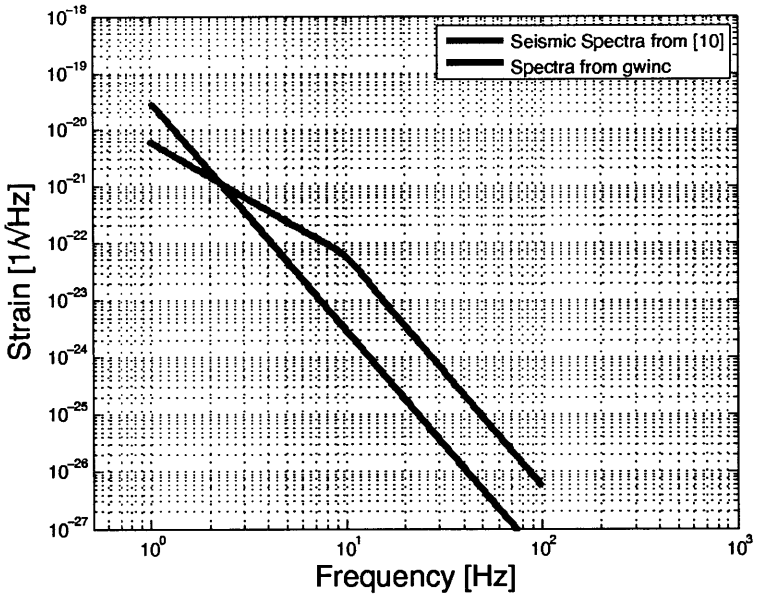

Figure 3-3: Plot of seismic Newtonian noise as per Equation 3.15 with ground motions from GWINC and [10].

actually corresponds reasonably well to the ground motion given in the `gravg.m` part of the GWINC MATLAB script [28]. Since the origin of the functional form of the ground spectra in `gravg` is unclear as no source is provided we plot using both this and the data we found. In `gravg` the ground motion is given by

$$\tilde{x}(f) = \frac{a}{1+3\Gamma(f-f_k)} + a\left(1 - \frac{1}{1+3\Gamma(f-f_a)}\right)\left(\frac{f_k}{f}\right)^2. \tag{3.16}$$

where the script gives the knee frequency $f_k = 10$ Hz, a low frequency level $a = 1 \times 10^{-9}$, $\Gamma = 0.8$, and $\beta = 0.6$.

3.2 Atmospheric Gravity Gradient Noise

We now present a theoretical estimate of the atmospheric Newtonian noise due to fluctuations of mass densities in the atmosphere generated by acoustic and turbulent phenomenon. We can continue the first half of the analysis performed in ?? as the derivation considered general regions of fluctuating mass without specifying seismic induced fluctuations until the latter half of the analysis. Thus we begin with Equation

3.7:

$$\left((\omega^2-\omega_0^2)^2+\omega^2/\tau^2\right)|x(\omega)|^2=\frac{4G^2}{3\pi^3 v_s^4}\omega^4|\Delta M(\omega)|^2. \tag{3.17}$$

Recall that this equation give us the force exerted on a test mass by local gravitational fluctuations and since LIGO measures the difference in the separations between test masses we must consider all four test masses. We argued that the forces induced by mass fluctuations around a test mass are largely dominated by local fluctuations, and thus we may add the contributions for any two test masses in quadrature. Similarly the two orthogonal arms of the interferometer are uncorrelated, so altogether the difference in sepoarations is four times the motion of an individual mass,

$$\left((\omega^2-\omega_0^2)^2+\omega^2/\tau^2\right)|x(\omega)|^2=\frac{16G^2}{3\pi^3 v_s^4}\omega^4|\Delta M(\omega)|^2. \tag{3.18}$$

In the previous analysis of seismic Newtonian noise we justified the absence of correlation of test masses from a short wavelength approximation based on S and P-waves. In this atmospheric estimation we consider the most disruptive atmospheric Newtonian noise to propagate at the speed of sound $c_s = 343$ m/s. Since the frequency range of the gravitational gradients we are considering is 1-10 Hz, this corresponds to values of wavelengths of 343 m to 34.3 m. The LIGO arm length is $L = 4$ km and thus we may consider the approximation $\lambda << L$ to be valid, and thus the atmospheric Newtonian noise in test masses can be considered uncorrelated.

Now we can cast 3.18 in terms of observables. Specifically we need to write $|\Delta M(\omega)|$ in terms of pressure fluctuations $|\Delta p(\omega)|$,

$$|\Delta M(\omega)|^2 = V^2|\Delta\rho(\omega)|^2 \tag{3.19}$$

where V is the volume of the coherent region and $\rho(\omega)$ is the frequency dependent density. Just as the quantity $G\rho X$ has dimensions of force per unit mass and we can thus equate $\omega^2 x = AG\rho X$, we may consider the same analysis for air pressure fluctuations. Measurements of air pressure give us the fractional pressure fluctuation $\Delta p/p$ and if the radius of a coherent region of fluctuating pressure is on the order

of λ, then we may equate $\omega^2 x = AG\rho\lambda\Delta p/p$, where A is another dimensionless constant. We also note that while evaluating $|\Delta M(\omega)|^2$ we are considering the rapid compression and expansion of a region of air. We may consider a process where that there is no opportunity for significant heat exchange, in other words an adiabatic process. What we are concerned with is the bulk modulus K, which measures the substance's resistance to uniform compression. For a gas, the adiabatic bulk modulus K_S is approximately given by $K_S = \gamma P$ where γ is the adiabatic index or heat capacity ratio. Since the pressure scales quadratically we must add a factor of $1/\gamma^2$ to account for the adiabatic compression of air. For dry air at 20° C, $\gamma = 1.400$. Thus $1/\gamma^2 = 0.51 \approx 1/2$. Considering coherent regions of $\lambda/2$ and rewriting $\rho(\omega)$ as $p(\omega)$ using the pressure and density of air, p_a and ρ_a, we can now write

$$|\Delta M(\omega)|^2 = \frac{1}{2}\left(\frac{\lambda}{2}\right)^6 \frac{\rho_a^2 |\Delta p(\omega)|^2}{p_a^2} = \frac{1}{2}\left(\frac{\pi v_s}{\omega}\right)^6 \frac{\rho_a^2}{p_a^2}|\Delta p(\omega)|^2. \tag{3.20}$$

Upon substitution into 3.18 we find

$$\left((\omega^2 - \omega_0^2)^2 + \omega^2/\tau^2\right)|x(\omega)|^2 = \frac{8\pi^3 G^2}{3}\frac{v_s^2}{\omega^2}\frac{\rho_a^2}{p_a^2}|\Delta p(\omega)|^2. \tag{3.21}$$

Now we reformulate this into a transfer function, making the same short wavelength approximation that allows us to ignore the resonance and damping of the test masses. Reformulating in terms of frequency f we find

$$|x(f)|^2 = \frac{8\pi^3 G^2}{3}\frac{v_s^2}{(2\pi f)^6}\frac{\rho_a^2}{p_a^2}|\Delta p(f)|^2. \tag{3.22}$$

We now provide a slightly different derivation, as similarly presented in [?], that gives the same result as what we just derived. The importance of this is that it will build the formalism we will need to perform the submerged calculation in the next chapter, but also we made many bold approximations in the previous derivation. Some of those approximations were justified for the seismic Newtonian noise calculation but less so for the atmospheric Newtonian noise calculation. This additional derivation will verify that we are on track and will lay the groundwork for the

calculation in the following chapter.

We consider a pressure wave propagating through a homogeneous air space at the speed of sound v_s. As the fractional pressure change is small it will induce the adiabatic density change $\delta\rho/\rho = \delta p/\gamma p$. The gravitational acceleration produced in the direction of propagation is

$$g = \int \frac{Gz\delta\rho}{r^3} dV. \tag{3.23}$$

Since there is only acceleration in the direction of propagation and not transverse and the detector is only concerned with motion parallel to the interferometer arms we pick up a factor of $\cos\theta$ just as in the previous derivation. Here is where we generalize the previous derivation to pressure fluctuations. The test mass is housed within some structure which suppresses noise which can be interpreted as a high frequency cutoff factor $C(2\pi f r_{min}/v_s)$. This provides some formalism to our discussion of the radius of coherent regions around a test mass. The function $C(x)$ depends on the shape of the structure and its acoustic properties, i.e. the ways in which it reflects sound. Based on these assumptions and without making bold approximations as before we can evaluate the integral as is done in [4] and [?],

$$g(t) = \int \frac{Gz\delta\rho}{r^3} dV = \frac{G\rho v_s}{\gamma p f} \cos\theta C(2\pi f r_{min}/v_s)\delta p(t + 1/4f). \tag{3.24}$$

Since $d^2h/dt^2 = g(t)/L$, or in the frequency domain $\tilde{h}(f) = g(t)/((2\pi f)^2 L)$ where L is the length of the interferometer arm. We find the strain signal in the interferometer to be

$$\tilde{h}(f) = \frac{Gv_s}{4\pi^2\gamma L}\frac{\rho}{p}\frac{1}{f^3} \cos\theta C(2\pi f r_{min}/v_s)\delta\tilde{\rho} \tag{3.25}$$

To simplify our equations and express them in a more meaningful way we want to write the noise as a spectral density $S(f)$, where the dimensionless strain noise would be $\sqrt{S(f)}$. In terms of $\tilde{h}(f)$, $S(f) = \langle\tilde{h}(f)\tilde{h}(f)^*\rangle = S(f)\delta(f - f')$. Thus we find

$$S(f) = \frac{G^2 v_s^2 \rho_a^2}{16\pi^4\gamma^2 L^2 p_1^2}\frac{1}{3f^6}\sum_{i=1}^{4} C(2\pi f r^i_{min}/v_s)^2 S^i_p(f). \tag{3.26}$$

where the index i sums over the test masses in the interferometer and r^i_{min} is the radius of the structure housing the i-th test mass. This result is essentially the same as what we had before except we made fewer assumptions about the correlation of the noise in each test mass and the exact nature of the coherent regions.

Chapter 4

Gravity Gradient Noise in a Submerged Detector

In order to extend the gravitational wave detection frequency below 10 Hz one needs to develop novel methods of reducing Newtonian noise because, as we have discussed, as isolation from seismic noise improves Newtonian noise will become the dominate noise source at low frequencies. Moreover it is calculated that this noise will exceed the expected gravitational wave signal below 10 Hz. Seismic and atmospheric induced fluctuations in gravitational fields directly couple to LIGO test masses, bypassing all stages of attenuation. Since no filter or shield can be built to prevent this direct coupling we must consider alternative approaches to reducing Newtonian noise. One consideration is to submerge an interferometric gravitational wave detector in some body of water. The hope would be that such a detector would experience reduced Newtonian noise from atmospheric sources as well as seismic sources.

4.1 Reductions in Atmospheric Newtonian Noise

We have setup up the necessary formalism in Chapter 3 to consider the effect of submerging an interferometric gravitational wave detector in some viscous fluid, like water. The path length difference fluctuations due to pressure fluctuations were calculated in 3.2. Thus we can perform a naive calculation of the equivalent Newtonian

noise from pressure fluctuations in water. The reason this calculation is naive is that in the atmospheric calculation we claimed that coherent regions of pressure fluctuations for each test mass were uncorrelated which we justified by a short wavelength approximation. More specifically the atmospheric Newtonian noise for a given test mass was dominated by the local regions of pressure fluctuations with coherence length $\lambda/2$, and since $L >> \lambda$ for arm length L this allowed us to add the noise in quadrature. In air the pressure fluctuations will not exceed the speed of sound $v_s = 343$ m/s, but in water the speed of sound is substantially higher. In fresh water at 25° C the speed of sound is 1497 m/s. For frequencies of 1 and 10 Hz this corresponds to wavelengths of 1500 m and 150 m. Since $L = 4$ km this approximation is no longer as valid.

Obviously most underwater disturbances do not propagate at the limiting velocity but what we can assume is that the atmospheric Newtonian noise for each test mass is correlated in submerged detectors. Additionally the correlation length for pressure waves at these frequencies will be much larger than for ground based detectors. This fact has an important implication, the gravity gradients will be correlated across the entire detector which will suppress their noise contribution, especially at lower frequencies. This fact indicates that we should see a decrease in atmospheric Newtonian noise, as we were hoping.

4.1.1 A Naive Calculation

We begin with a naive calculation in the same vein as the one outlined in Chapter 3. We already admitted that the pressure fluctuations are more correlated due to increased pressure wave propagation velocities. But we will first perform the calculation of the noise using the short wavelength approximation and subsequently consider a more rigorous approach. This can be interpreted as the noise in a submerged detector with ideal uncorrelated pressure fluctuations. We start with Equation 3.22 as derived in Section 3.2

$$\left((\omega^2 - \omega_0^2)^2 + \omega^2/\tau^2\right) |\Delta x(\omega)|^2 = \frac{8\pi^3 G^2}{3\gamma^2} \frac{v_s^2}{\omega^2} \frac{\rho_w^2}{p_w^2} |\Delta p(\omega)|^2. \tag{4.1}$$

Ignoring the resonant frequency and damping time of the test mass, as we previously justified, and expressing the noise spectra in terms of frequency f, we find that

$$|\Delta x(f)|^2 = \frac{8\pi^3 G^2}{3\gamma^2} \frac{v_s^2}{(2\pi f)^6} \frac{\rho_w^2}{p_w^2} |\Delta p(f)|^2. \tag{4.2}$$

where we now have v_s as the speed of sound in water, p_a the water pressure, which is dependent on depth, and ρ_w which is 998.2 kg/m^3 at 20° C and approaches 999 kg/m^2 as the water temperature approaches 0° C. Lastly, γ is the adiabatic index which arises from the adiabatic compression of a fluid; for H_2O at 20° C, $\gamma = 1.330$. To simplify our equations and express them in a more meaningful way we want to write the noise as a spectral density $S(f)$, where the dimensionless strain noise would be $\sqrt{S(f)}$. We also write $|\Delta p(f)|^2$ as the acoustic noise spectral density $S_p(f)$. We now find an L^2 in the denominator where L is the interferometer arm length. We now have

$$S(f) = \frac{G^2 v_s^2 \rho_w^2}{24\pi^3 \gamma^2 L^2 p_w^2} \frac{1}{f^6} S_p(f). \tag{4.3}$$

4.1.2 Results

We now want to find the power spectra of acoustic noise. We investigated many studies of acoustic ambient noise in the ocean and extrapolating from collected data we estimate an acoustic ambient noise power spectra. The data on which we are basing our power spectra is from [1], [3], [6], [11], [17], [21], and [33].

Careful analysis of the seven sources we cited gives us a feel for the ambient noise due to pressure perturbations in the ocean. It turns out the ranges in ambient acoustic noise determine whether or not we see an improvement. Considering the lowest noise floor observed in the power spectra there is a minor improvement over the atmospheric Newtonian noise experienced in ground based detectors. But if we consider the average of the power spectra for ambient acoustic noise in deep ocean, there is no improvement as the ambient noise is too loud. We estimated the frequency dependence in the power spectra for ambient acoustic noise to be $1/f^2$, on a loglog plot. This was fairly typical of frequencies 1-100 Hz, although only a few sources provided

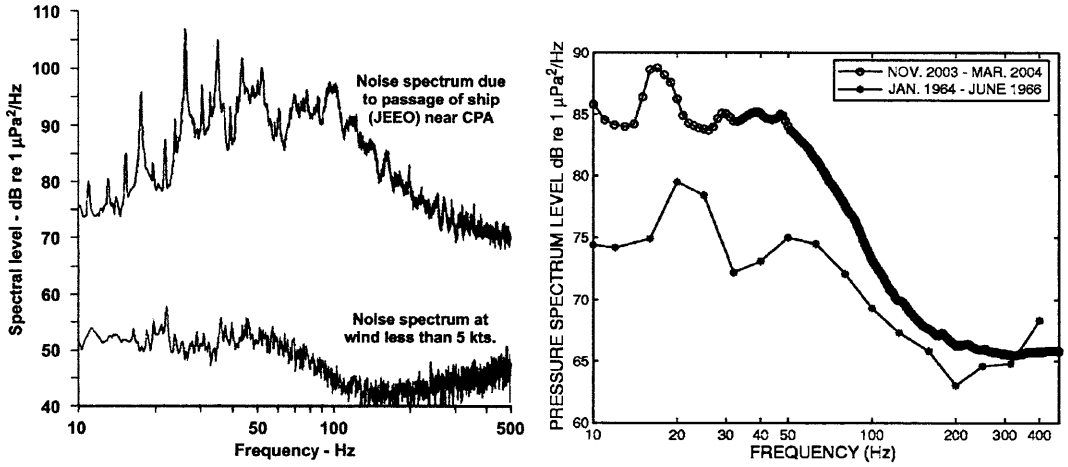

Figure 4-1: Examples of ambient noise in the ocean, on the left deep ocean ambient noise in the Northeast Pacific, modified from [11], and on the right North Pacific west of California, modified from [17].

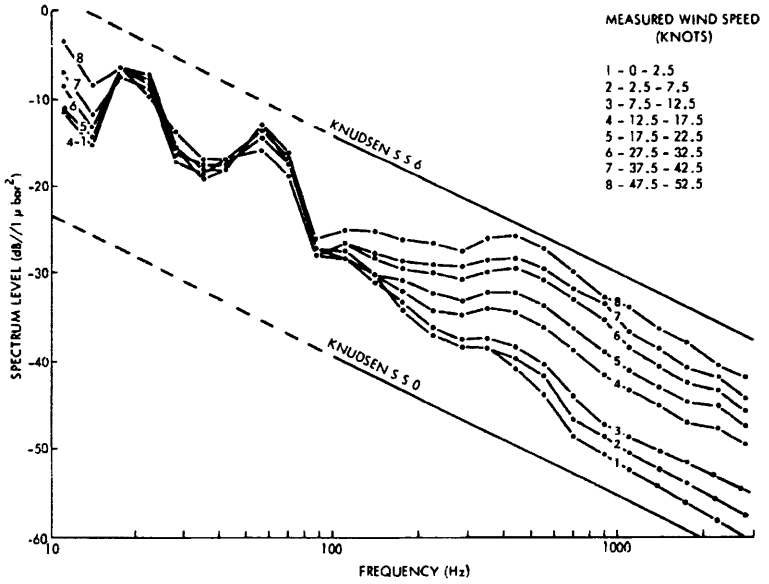

Figure 4-2: Variation of deep ocean ambient noise in the Northwest Atlantic with respect to wind speed, Modified from [21].

information below 10 Hz. A few constants of proportionality were determined for the acoustic noise based on the cited sources, corresponding to an average noise floor, which averaged the constants determined for all the sources, a relatively quiet noise floor where the a few of the quietest results were considered from the sources, and a constant corresponding to the two quietest ambient acoustic noise floors observed in the cited studies. A few of the power spectra for deep ocean ambient acoustic noise are shown in Figure 4-2. The units on the ordinate axis are dB *re* $1\mu\text{Pa}^2/\text{Hz}$, or some similar variant. These are magnitude with respect to some reference unit, which in the one stated is $1\mu\text{Pa}^2/\text{Hz}$. The conversion to a pressure in units of $\mu\text{Pa}^2/\text{Hz}$ is done using

$$\text{dB} = 10\log_{10}\left(\frac{p}{1\mu\text{Pa}^2/\text{Hz}}\right). \tag{4.4}$$

Having determined the transfer function for ambient acoustic noise we plot the atmospheric Newtonian noise curves in contrast with atmospheric Newtonian noise in air, the Newtonian noise in Advanced LIGO, and the LIGO noise curve. A few plots are shown and discussed in Figure . We see that if a interferometric gravitational wave detector were constructed underwater the atmospheric noise levels would be comparable to those in ground based detectors, and far below the total Advanced LIGO noise curve.

An important fact to keep in mind is that this was a naive calculation done using a short wavelength approximation, and thus we should assume that since we assumed that all coherently fluctuating regions were uncorrelated and the only contribution to the noise at the test mass was from the pressure fluctuations adjacent to it. For ground based detectors, where $v_s = 343$ m/s, this would be a valid approximation, but for a submerged detector, where $v_s = 1500$ m/s, concerning the frequency range 1 to 10 Hz this is an over approximation, which means the atmospheric contribution to Newtonian noise would be even lower than the level seen in our results.

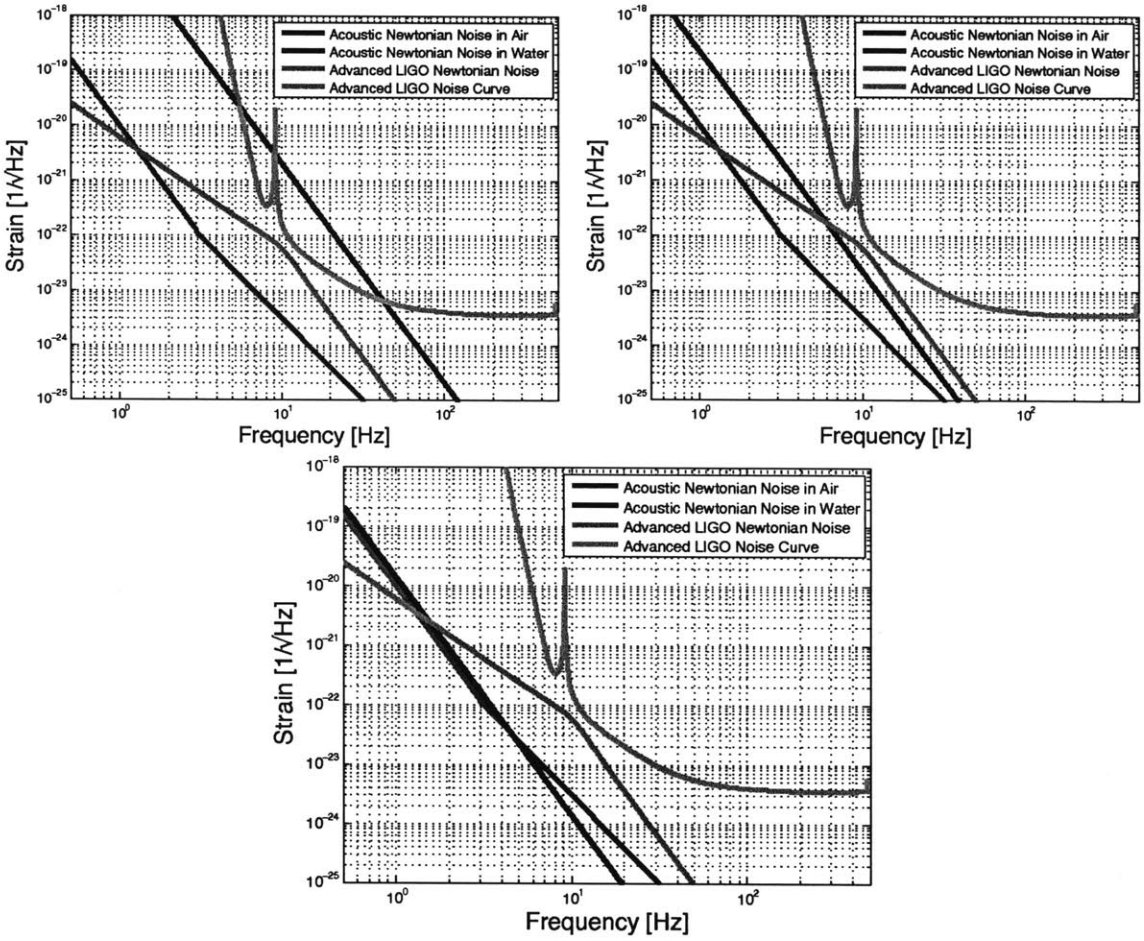

Figure 4-3: Clockwise from the top left: Acoustic Newtonian noise at depth of 100 meters and with a constant of proportionality corresponding to average ambient noise, acoustic Newtonian noise at depth of 1000 meters and with a constant of proportionality corresponding to a relatively quiet ambient noise, and acoustic Newtonian noise at depth of 1000 meters and with a constant of proportionality corresponding to the quietest acoustic ambient noise.

4.1.3 A Long Wavelength Approximation

We now consider density fluctuations where the characteristic length of the coherent pressure fluctuation is larger than the interferometer arm length $\lambda >> L$. In this scenario the effect of a gravitational gradient in an interferometer is not the incoherent sum of the gravitational forces exerted by the density or pressure fluctuations experienced by the test masses, added in quadrature. But instead there is a fluctuation in the gravitational field across the entirety of the interferometer. Therefore we must be explicit in how we consider that forces on each test mass ass opposed to just adding in quadrature. We must consider the difference in the gradient at each test mass due to the fluctuation. So we develop some formalism to this. The differential length change in the interferometer is

$$\delta L = h(t)L = \left(x^{(3)} - x^{(4)}\right) - \left(y^{(2)} - y^{(1)}\right) \tag{4.5}$$

where the index indicates the test mass. Moving down the y arm and over the x arm we label the test masses in succession, as in the corner mass on the x arm is mass 4 and the inner mass on the y arm is mass 2. Clearly x and y correspond to the positions of the respective test mass, thus we can see how the differential length change arises from test mass motion. If the signal is induced by some density or pressure fluctuation then $h(t)$ is the Newtonian noise signal. In terms of accelerations we have

$$\frac{d^2h(t)}{dt^2} = \frac{1}{L}\left(\left(a_x^{(3)} - a_x^{(4)}\right) - \left(a_y^{(2)} - a_y^{(1)}\right)\right) \tag{4.6}$$

where the a's correspond to the components of the acceleration experienced by the respective test mass. In the frequency domain this is equivalent to

$$\tilde{h}(f) = -\frac{1}{L(2\pi f)^2}\left(\left(\tilde{a}_x^{(3)} - \tilde{a}_x^{(4)}\right) - \left(\tilde{a}_y^{(2)} - \tilde{a}_y^{(1)}\right)\right) \tag{4.7}$$

Since the density and pressure fluctuations constitute a stochastic process we know that the spectral density should be $S(f) = \langle \tilde{h}(f)\tilde{h}(f)^* \rangle$, which amounts to

$$S(f) = -\frac{1}{L(2\pi f)^2} \left\langle \left| \left(\tilde{a}_x^{(3)} - \tilde{a}_x^{(4)}\right) - \left(\tilde{a}_y^{(2)} - \tilde{a}_y^{(1)}\right) \right|^2 \right\rangle. \tag{4.8}$$

where we have not assumed anything about the nature of the fluctuation's characteristic coherence length or correlations in signal.

It is clear that the quantity we are interested in is the difference in accelerations. We can calculate this considering a long wavelength approximation and resorting back to the simplified model and diagram in Figure 3-1. Recall that we found for some region of fluctuating mass the acceleration experienced by the test mass is

$$a = G\Delta M(f)\frac{\cos\theta}{r^2}. \tag{4.9}$$

Recall that in our initial analysis we had to consider the sum of coherently fluctuating regions $\sum \cos^2\theta/r^4$ with some inner cutoff radius. The analogous terms here is calculated from $(a_x^{(0)} - a_x^{(1)}) - (a_y^{(0)} - a_y^{(2)})$, where we have reindexed to conform to the simplified model. From the diagram in Figure 3-1 two terms become immediately clear

$$a_x^{(0)} = G\Delta M(f)\frac{\cos\theta}{r^2} \quad a_y^{(0)} = -G\Delta M(f)\frac{\sin\theta}{r^2} \tag{4.10}$$

Consider mass one on the x axis, call the distance to the mass perturbation c and the angle internal to the interferometer γ, from the law of cosines and law of sines we find $c^2 = r^2 + L^2 - 2rL\cos\theta$ and $\sin\gamma = r/c\sin\theta$. Equivalently for the corner mass on the y axis $d^2 = r^2 + L^2 - 2rL\sin\theta$ and $\sin\sigma = r/d\cos\theta$. Thus we find

$$a_x^{(1)} = G\Delta M\frac{\cos(\gamma)}{c^2} \quad a_y^{(2)} = -G\Delta M\frac{\cos(\sigma)}{d^2} \tag{4.11}$$

We now perform a series expansion on our expression for $(a_x^{(0)} - a_x^{(1)}) - (a_y^{(0)} - a_y^{(2)})$ to the first order in L. We use this approximation because the distance to the fluctuating region is r, since we imposed some inner cutoff at which no longer contribute which

was on the order of $r \sim \lambda$, thus $r >> L$. So expanding the the first order in L should be sufficient. The leading order term cancels out and we are left with

$$\frac{3G\Delta ML}{r^3}(\sin^2\theta - \cos^2\theta). \tag{4.12}$$

We find the summation over all contributing regions of coherent fluctuation by integrating r from r_{min} to ∞ and over all θ, doing so we find

$$\sum \frac{9G^2L^2}{r^6}(\sin^2\theta - \cos^2\theta)^2 \approx \frac{144G^2L^2\omega^6}{5\pi^5 v_s^6} \tag{4.13}$$

since $r_{min} = \lambda/4$ and $\lambda = 2\pi v_s/\omega$. For pressure fluctuations we know that

$$|\Delta M(\omega)|^2 = \frac{\pi^6 v_s^6}{\gamma^2}\frac{\rho^2}{p^2\omega^6}|\Delta p(\omega)|^2. \tag{4.14}$$

The acoustic noise spectra is for coherent pressure fluctuations with a long characteristic wavelength is

$$S(f) = \frac{144\pi G^2}{5\gamma^2}\frac{\rho^2}{p^2}S_p(f). \tag{4.15}$$

Considering our interferometric gravitational wave detector submerged in water, where the speed of sound is $v_s = 1500$ m/s, we can expect that below 0.1 Hz, the acoustic spectra will go as 4.15. As there have been no deep ocean acoustic noise studies in sub 1 Hz frequency range we cannot plot the resulting spectra but the functional form and dependence on parameters, or lack thereof, gives us an idea of the low frequency behavior.

4.2 Reductions in Seismic Newtonian Noise

We have seen that in the ideal case where we construct an interferometer in the parts of the ocean with the lowest ambient acoustic noise and that there is not an increase in the atmospheric noise. An improvement comes with the absence of the seismic noise experienced on the surface in ground based detectors. As discussed in [13] the major contributions to seismic Newtonian noise is from density fluctuations due to surface

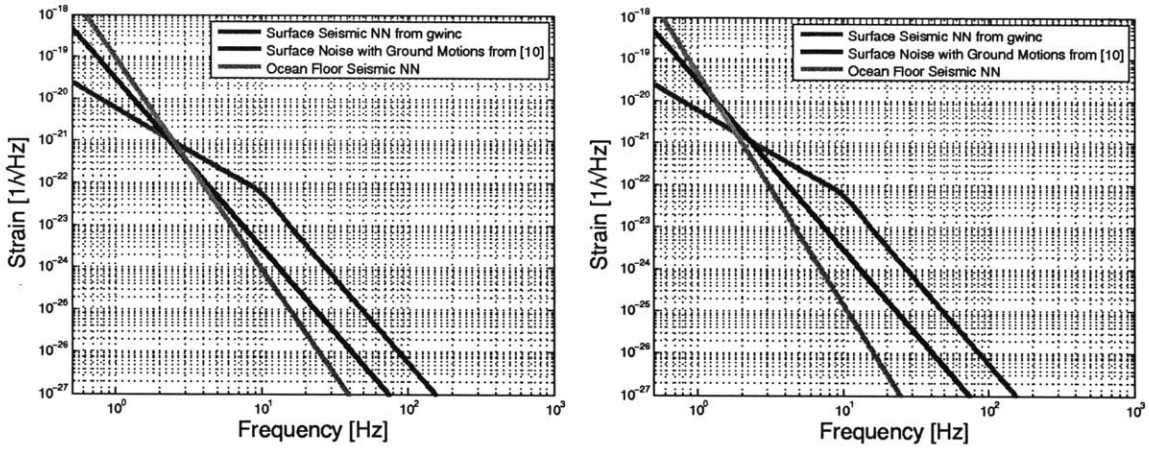

Figure 4-4: Seismic Newtonian noise on the surface compared to that on the ocean floor. On the left is an average ambient seismic noise on the ground and on the right is a quiet ambient seismic noise on the ocean floor.

waves, i.e. Rayleigh and Love modes, and these do not exist at the same strength in the ocean as on the surface. Previously we calculated the seismic Newtonian noise as generated by `gwinc.m` as well as our own study of seismic noises on the surface as presented in [10]. We consider the same expression for the seismic noise, a strain as a function of the ground motions,

$$\tilde{h}(f) = \frac{G\rho_e\beta}{L\pi}\frac{1}{f^2}\tilde{x}(f), \tag{4.16}$$

where ρ_e is now the density of the surface of the ocean floor which is approximately $\rho_e \approx 3000$ kg/m^3, assuming the ocean floor is largely composed of basaltic rock. We now need to determine the spectrum for seismic noise on the ocean floor. We use the broadband ambient seismic noise studies done in [?] and [?] which gives ocean floor seismic spectra from different points in oceans around the world. As we did with pressure fluctuations we look through the various spectra and determine a dependence on frequency on a loglog plot and then determine constants of proportionality for an average of the spectra and then for the least noisy of the spectra. The results are plotted in Figure 5-1.

Since the short wavelength approximation that led to 4.16 is a good approximation we can assume that this is not an overestimate of the seismic Newtonian noise. We

see that in fact on the ocean floor the seismic Newtonian noise is lower than the seismic Newtonian noise experienced in ground based interferometric gravitational wave detectors as per our calculation using ambient surface seismic data from [10] and the Newtonian noise produced by `gwinc.m`. This has two important consequences for submerged detectors; the seismic noise is lower on the ocean floor than on the surface, thus seismic isolation, which is currently still a limiting noise source in Advanced LIGO, would improve in a submerged detector. Moreover since the decrease in seismic noise has resulted in a decrease in the seismic Newtonian noise compared to that in ground based detectors.

Chapter 5

Conclusions and Future Work

We derived a number of formalisms and methods to express Newtonian noise in more general ways. The work relied heavily upon work already done in [25], [?], [13], and [4], but also expanded upon their work in seemingly unique ways. After developing the formalism for discussing Newtonian noise from seismically induced density fluctuations and atmospheric pressure fluctuations from acoustic and turbulent phenomena we considered ways to reduce the Newtonian noise in next generation interferometric gravitational wave detectors.

As methods for seismic isolation in LIGO detectors improve the sensitivity below 10 Hz will be increasingly inhibited by gravity gradient noise. There are no direct methods of screening out this noise as gravitational fields couples directly to mass and thus the noise directly to the test masses. One can not in principle measure the gravity gradient noise in a detector and subtract it because measuring the Newtonian noise would constitute measuring changes in the gravitational field. This is analogous to constructing a gravitational wave detector because detection of gravitational waves is, in fact, a measurement of the changes in a gravitational field. Thus a detector at such a sensitivity would nullify the need for an interferometer.

Although there have been efforts to model the Newtonian noise and subtract it from the signal doing so requires very low levels of seismic activity and extremely precise knowledge of the seismic activity that does occur. The proposal in [2] would require construction of an underground detector. The next consideration is the con-

struction of a detector where we can expect reductions in both types of Newtonian noise. We considered the construction of a submerged interferometric gravitational wave detector. These postulations are not assertions that we should construct underwater gravitational wave detectors, but rather ways to look and gain a better understanding of Newtonian noise. Although the unsure fate of LISA raises questions about the where the future of gravitational wave detection lies.

We first derived the power spectra of Newtonian noise in terms of ambient pressure fluctuations and after compiling various deep sea ambient noise studies we presented the resulting spectra for atmospheric Newtonian noise from pressure fluctuations at various depths and with varying levels of ambient noise. Additionally we looked at the validity of our short wavelength approximation and subsequently performed a long wavelength approximation in order to better determine the Newtonian noise from pressure fluctuations. We also derived the Newtonian noise from seismic activity and applied the result to the ocean floor. After analyzing a few studies of ambient noise levels on the ocean floor we determined the associated Newtonian noise. We found that the seismic noise on the ocean floor was lower than that on the surface, which has beneficial implications for seismic isolation in submerged detectors. More importantly the Newtonian noise from seismic activity was subsequently lower for a detector on the ocean floor.

We also found that the Newtonian noise from pressure fluctuations in submerged detectors could be lower than that in ground based detectors, but depended on the depth and ambient noise levels. The ambient noise for pressure fluctuations seemed to vary depending on one's location in the ocean, but given the choice of a quiet location in the ocean and sufficient depth the Newtonian noise is on the same order of magnitude as for ground based detectors. We argued that our approximation was an overestimate of the Newtonian noise due to the breakdown of the short wavelength approximation underwater. This leads to an overestimation because we considered the coherent regions of pressure fluctuations around each test mass and added them in quadrature. But as these coherent regions become larger, as the v_s in water is greater than in air, they begin to overlap. Note that for a stochastic process like pressure

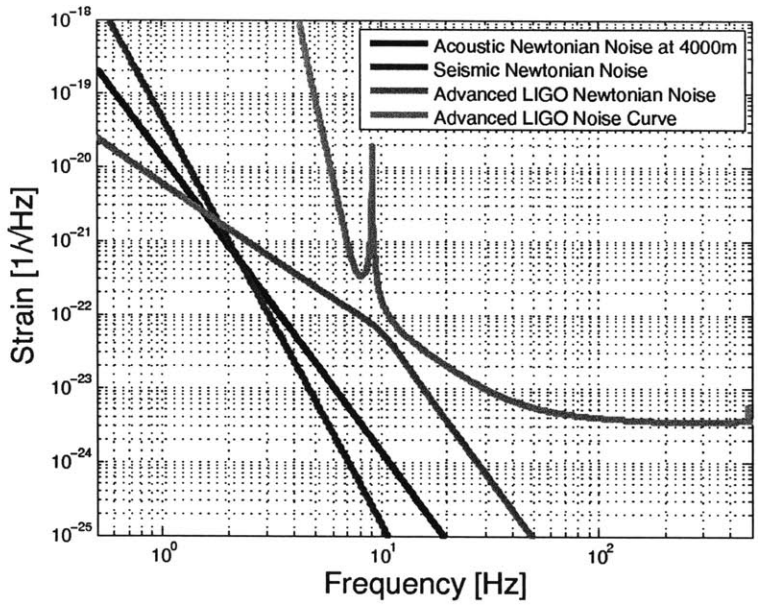

Figure 5-1: The Newtonian noise from pressure fluctuations and seismic activity in a submerged detector, on the ocean floor at a depth of 4000m.

fluctuations the correlation of these regions will not amplify the signal. So we are considering coherent regions that overlap and thus overestimating the Newtonian noise from pressure fluctuations. This implies that the actual contributions will be lower than what we calculate.

So the ideal submerged interferometric gravitational wave detector could be on the ocean floor. Considering a depth of 4000 m, which is the average depth of the Pacific ocean, we present the resulting Newtonian noise from both pressure fluctuations and seismic activity. The results are shown in Figure 5-1.

Additional work that could be done includes accounting for atmospheric Newtonian noise without using short or long wavelength approximations but instead calculating the correlation function between coherent regions. Additionally there might be a number of additional contributions to the Newtonian noise in a submerged detector that we might need to account for. Specifically it is possible that temperature fluctuations in the ocean would contribute to pressure fluctuations, increasing the associated atmospheric Newtonian noise.

We have presented an initial analysis of the sources of Newtonian noise that would exist in a submerged interferometric gravitational wave detector and considering ideal

ambient pressure and seismic noise we would likely see an improvement in the Newtonian noise that limits low frequency detection in Advanced LIGO.

Appendix A

Reduced Transfer Functions

Recall that the reduced transfer function for a mode J is $\beta_J = \gamma_J \Gamma_J \beta'_J$. The attenuation of the gravity gradient due to a height h above the Earth's surface is described as $\Gamma_J = \exp(-\omega H/v_{sJ})$, where v_{sJ} is the phase velocity of the J mode. For LIGO test masses $H \sim 1.5$ m, the frequency of greatest concern might be $f \approx 10$ Hz and we can assume that the dominant contributor to the noise in from the fundamental Rayleigh mode, which for 10 Hz corresponds to $v_s \simeq 330$ m/s [13]. This gives us the attenuation factor of $\Gamma \simeq 0.75$ for the fundamental Rayleigh mode. For all other modes the v_s associated with that mode will be higher and thus the attenuation factor will be much closer to unity. So our approximation of $\Gamma \sim 1$ was not an unreasonable approximation.

To help provide a connection between the work done in Chapter 3 and the actual seismic Newtonian noise experiance at the LIGO detectors we present the reduced transfer functions predicted for the Livingston and Hanford LIGO sites, as calculated in [13]. Shown are the ranges of β' for different models of fundamental Rayleigh modes. Also shown are the range of reduced transfer functions β'_L which corresponds to models where the Rayleigh modes are considered alongside Love modes. If enough Love modes mix with each Rayleigh mode then mode's anisotropy ratio, which can be fairly high, would be reduced to an anisotropy ratio at the level of quiet times at the LIGO sites. Values of the two reduced transfer functions discussed, $beta'$ and β'_L are given in Table A.1.

Table A.1: The reduced transfer functions β' predicted for the Hanford and Livingston sites, as calculated in [13], contrasted with our original estimate for β.

Original Derivation $\beta = 1/\sqrt{3} = 0.577$				
Modes	Hanford β'	Hanford β'_L	Livingston β'	Livingston β'_L
RF $f < 10$ Hz	0.4-0.85	0.35-0.6	0.65-0.9	0.35-0.45
RF $f > 10$ Hz	0.85	0.6	0.65-0.9	0.35-0.45
RS	0.4-1.4	0.35-0.6	0.0-1.2	0.0-0.9
RP	0.0-0.15	0.0-0.15	0.02-0.13	0.01-0.06

Bibliography

[1] R. K. Andrew, B. M. Howe, J. A. Mercer, and M. A. Dzieciuch. Ocean ambient sound: Comparing the 1960s with the 1990s for a receiver off the california coast. *Acoustics Research Letters Online*, 3(2):65–70, 2002.

[2] M. Beker, G. Cella, R. DeSalvo, M. Doets, H. Grote, J. Harms, E. Hennes, V. Mandic, D. Rabeling, J. van den Brand, and C. van Leeuwen. Improving the sensitivity of future gw observatories in the 110 hz band: Newtonian and seismic noise. *General Relativity and Gravitation*, 43:623–656, 2011. 10.1007/s10714-010-1011-7.

[3] M. J. Buckingham. On surface-generated ambient noise in an upward refracting ocean. *Philosophical Transactions: Physical Sciences and Engineering*, 346(1680):pp. 321–352, 1994.

[4] C. Cafaro and S. A. Ali. Analytical Estimate of Atmospheric Newtonian Noise Generated by Acoustic and Turbulent Phenomena in Laser-Interferometric Gravitational Waves Detectors. 2009.

[5] S. Carroll. *Spacetime and Geometry: An Introduction to General Relativity.* Addison Wesley, 2004.

[6] N. R. Chapman and J. W. Cornish. Wind dependence of deep ocean ambient noise at low frequencies. *The Journal of the Acoustical Society of America*, 93(2):782–789, 1993.

[7] T. Corbitt et al. A squeezed state source using radiation pressure induced rigidity. 2005.

[8] T. Creighton. Tumbleweeds and airborne gravitational noise sources for LIGO. *Class. Quant. Grav.*, 25:125011, 2008.

[9] S. Dimopoulos, P. W. Graham, J. M. Hogan, M. A. Kasevich, and S. Rajendran. An Atomic Gravitational Wave Interferometric Sensor (AGIS). *Phys. Rev.*, D78:122002, 2008.

[10] J. E. Fix. Ambient Earth motion in the period range from 0.1 to 2560 sec. *Bulletin of the Seismological Society of America*, 62(6):1752–1760, 2008.

[11] R. Gaul, D. Knobles, J. Shooter, and A. Wittenborn. Ambient noise analysis of deep-ocean measurements in the northeast pacific. *Oceanic Engineering, IEEE Journal of*, 32(2):497 –512, april 2007.

[12] M. A. H. Hedlin and J. A. Orcutt. A comparative study of island, seafloor, and subseafloor ambient noise levels. *Bulletin of the Seismological Society of America*, 79(1):172–179, 1989.

[13] S. A. Hughes and K. S. Thorne. Seismic gravity-gradient noise in interferometric gravitational-wave detectors. *Phys. Rev.*, D58:122002, 1998.

[14] R. A. Hulse and J. H. Taylor. Discovery of a pulsar in a binary system. *Astrophys. J.*, 195:L51–L53, 1975.

[15] T. T. Lyons, M. W. Regehr, and F. J. Raab. Shot noise in gravitational-wave detectors with fabry-perot arms. *Appl. Opt.*, 39(36):6761–6770, Dec 2000.

[16] N. Mavalvala et al. Lasers and optics: Looking towards third generation gravitational wave detectors. *Gen. Rel. Grav.*, 43:569–592, 2011.

[17] M. A. McDonald, J. A. Hildebrand, and S. M. Wiggins. Increases in deep ocean ambient noise in the northeast pacific west of san nicolas island, california. *The Journal of the Acoustical Society of America*, 120(2):711–718, 2006.

[18] J. M. McGuirk, G. T. Foster, J. B. Fixler, M. J. Snadden, and M. A. Kasevich. Sensitive absolute-gravity gradiometry using atom interferometry. *Phys. Rev. A*, 65(3):033608, Feb 2002.

[19] M. V. Moody, H. A. Chan, and H. J. Paik. Superconducting gravity gradiometer for space and terrestrial applications. *Journal of Applied Physics*, 60(12):4308–4315, 1986.

[20] M. V. Moody, H. J. Paik, and E. R. Canavan. Three-axis superconducting gravity gradiometer for sensitive gravity experiments. *Review of Scientific Instruments*, 73(11):3957–3974, 2002.

[21] A. J. Perrone. Deep-ocean ambient-noise spectra in the northwest atlantic. *The Journal of the Acoustical Society of America*, 46(3B):762–770, 1969.

[22] J. Peterson. Observations and modeling of seismic background noise. *US Geol. Surv. Open-File Rept.*, 93, 1993.

[23] M. Pitkin, S. Reid, S. Rowan, and J. Hough. Gravitational Wave Detection by Interferometry (Ground and Space). 2011.

[24] P. Saulson. *Fundamentals of Interferometric Gravitational Wave Detectors.* World Scientific, 1994.

[25] P. R. Saulson. Terrestrial gravitational noise on a gravitational wave antenna. *Phys. Rev. D*, 30(4):732–736, Aug 1984.

[26] B. F. Schutz. Gravitational wave astronomy. *Class. Quant. Grav.*, 16:A131–A156, 1999.

[27] D. Shoemaker and the LSC. A comprehensive overview of advanced ligo.

[28] The LIGO Scientific Collaboration. GWINC (Gravitational Wave Interferometer Noise Calculator), MATLAB script: accepts as input a parameters that describe a Fabrey-Perot Cavity laser interferometer gravitational wave detector and estimates the limiting noises.

[29] K. S. Thorne and C. J. Winstein. Human gravity-gradient noise in interferometric gravitational-wave detectors. *Phys. Rev.*, D60:082001, 1999.

[30] R. Wald. *General Relativity.* Physics/Astrophysics. University of Chicago Press, 1984.

[31] S. J. Waldman. The Advanced LIGO Gravitational Wave Detector. 2011.

[32] S. C. Webb. Broadband seismology and noise under the ocean. *Reviews of Geophysics*, 36(1):105–142, 1998.

[33] G. M. Wenz. Acoustic ambient noise in the ocean: Spectra and sources. *The Journal of the Acoustical Society of America*, 34(12):1936–1956, 1962.